Variability and stability of anthropogenic CO2 in Antarctic Bottom Waters observed in the Indian sector of the Southern Ocean, 1978-2018

Léo Mahieu[1], Claire Lo Monaco[2], Nicolas Metzl[2], Jonathan Fin[2], Claude Mignon[2]

[1]Ocean Sciences, School of Environmental Sciences, 4 Brownlow Street, Liverpool L69 3GP, UK

[2]LOCEAN-IPSL, Sorbonne Université, CNRS/IRD/MNHN Paris, France

Correspondence to: Léo Mahieu (Leo.Mahieu@live.fr); Claire Lo Monaco (claire.lomonaco@locean.upmc.fr)

Abstract

Antarctic bottom waters (AABWs) are known as a long term sink for anthropogenic CO_2 (C_{ant}) but is hardly quantified because of the scarcity of the observations, specifically at an interannual scale. We present in this manuscript an original dataset combining 40 years of carbonate system observations in the Indian sector of the Southern Ocean (Enderby Basin) to evaluate and interpret the interannual variability of C_{ant} in the AABW. This investigation is based on regular observations collected at the same location (63° E/56.5° S) in the frame of the French observatory OISO from 1998 to 2018 extended by GEOSECS and INDIGO observations (1978, 1985 and 1987).

At this location the main sources of AABW sampled is the fresh and younger Cape Darnley Bottom Water (CDBW) and the Weddell Sea Deep Water (WSDW). Our calculations reveal that C_{ant} concentrations increased significantly in the AABW, from the average concentration of 7 µmol.kg^{-1} calculated for the period 1978-1987 to the average concentration of 13 µmol.kg^{-1} for the period 2010-2018. This is comparable to previous estimates in other SO basins, with the exception of bottom waters close to their formation sites where C_{ant} concentrations are about twice as large. Our analysis shows that total carbon (C_T) and C_{ant} increasing rates in the AABW are about the same over the period 1978-2018, and we conclude that the long-term change in C_T is mainly due to the uptake of C_{ant} in the different formation regions. This is, however, modulated by significant interannual to multi-annual variability associated with variations in hydrological (potential temperature (Θ), salinity (S)) and biogeochemical (C_T, total alkalinity (A_T), dissolved oxygen (O_2)) properties. A surprising result is the apparent stability of C_{ant} concentrations in recent years despite the increase in C_T and the gradual acceleration of atmospheric CO_2.

The C_{ant} sequestration by AABWs is more variable than expected and depends on a complex combination of physical, chemical and biological processes at the formation sites and during the transit of the different AABWs. The interannual variability at play in AABWs needs to be carefully considered on the extrapolated estimation of C_{ant} sequestration based on sparse observations over several years.

1 Introduction

Carbon dioxide (CO_2) atmospheric concentration has been increasing since the start of the industrialization (Keeling and Whorf, 2000). This increase leads to an ocean uptake of about a quarter of C_{ant} emissions (Le Quéré et al., 2018; Gruber et al., 2019a). It is widely acknowledged that the Southern Ocean (SO) is responsible for 40

% of the C_{ant} ocean sequestration (Matear, 2001; Orr et al., 2001; McNeil et al., 2003; Gruber et al., 2009; Khatiwala et al., 2009). Ocean C_{ant} uptake and sequestration have the benefit to limit the atmospheric CO_2 increase but also result in a gradual decrease of the ocean pH (Gattuso and Hansson, 2011; Jiang et al., 2019). Understanding the oceanic C_{ant} sequestration and its variability is of major importance to predict future atmospheric CO_2 concentrations, impact on the climate and impact of the pH change on marine ecosystems (de Baar, 1992; Orr et al., 2005; Ridgwell and Zeebe, 2005).

C_{ant} in seawater cannot be measured directly and the evaluation of the relatively small C_{ant} signal from the total inorganic dissolved carbon (C_T; around 3 %; Pardo et al, 2014) is still a challenge to overcome. Different approaches have been developed in the last 40 years to quantify C_{ant} concentrations in the oceans. The 'historical' back calculation method based on C_T measurement and preformed inorganic carbon estimate (C^0) was independently published by Brewer (1978) and Chen and Millero (1979). This method has been often applied at regional and basin scale (Chen, 1982; Poisson and Chen, 1987; Chen, 1992; Goyet et al., 1998; Körtzinger et al., 1998, 1999; Lo Monaco et al., 2005a). More recently the TrOCA method (Tracer combining Oxygen, dissolved Carbon and total Alkalinity) has been developed (Touratier and Goyet, 2004a, b; Touratier et al., 2007) and applied in various regions including the SO (e.g. Lo Monaco et al., 2005b; Sandrini et al., 2007; Van Heuven et al., 2011; Pardo et al., 2014; Shadwick et al., 2014; Roden et al., 2016; Kerr et al., 2018). Comparisons with other data-based methods show significant differences in C_{ant} concentrations, especially at high latitudes and more particularly in deep and bottom waters (Lo Monaco et al., 2005b; Vázquez-Rodríguez et al., 2009; Pardo et al., 2014). Thus, there is a need to better explore the C_T and C_{ant} temporal variability in the deep ocean, especially in the SO where observations are relatively sparse.

Antarctic bottom waters (AABWs) are of specific interest for the atmospheric CO_2 and heat regulation as they play a major role in the meridional overturning circulation (Johnson et al., 2008; Marshall and Speer, 2012). AABWs represent a large volume of water by covering the majority of the bottom world ocean (Mantyla and Reid, 1995), and their spreading in the interior ocean through circulation and water mixing is a key mechanism for the long-term sequestration of C_{ant} and climate regulation (Siegenthaler and Sarmiento, 1993). The AABW formation is a specific process occurring in few locations around the Antarctic continent (Orsi et al., 1999). In short, the AABW formation occurs when the Antarctic surface waters flows down along the continental shelf. The Antarctic surface waters density required for this process to happen is reached by the increase in salinity (S) due to brine release from the ice formation and by a decrease in temperature due to heat loss to either the ice-shelf or the atmosphere. Importantly, AABW formation process is enhanced by katabatic winds that open areas free of ice called polynyas (Williams et al., 2007). Indeed, katabatic winds are responsible for an intense cooling that enhance the formation of ice constantly pushed away by the wind, leading to cold and salty surface waters in contact with the atmosphere. The variable conditions of wind, ice production, surface water cooling and continental slope shape encountered around the Antarctic continent lead to different types of AABW, hence the AABW characteristics can be used to identify their formation sites.

The ability of AABW to accumulate C_{ant} has been controversial since one can believe that the ice coverage limits the invasion of C_{ant} in Antarctic surface waters (e.g. Poisson and Chen, 1987). This is, however, not the case in polynyas, and several studies have reported significant C_{ant} signals in AABW formation regions, likely due to the uptake of CO_2 induced by high primary production (Sandrini et al., 2007; van Heuven et al., 2011, 2014; Shadwick et al., 2014; Roden et al., 2016). However, little is known about the variability and evolution of the CO_2 fluxes in

AABW formation regions, and since biological and physical processes are strongly impacted by seasonal and interannual climatic variations (Fukamachi et al., 2000; Gordon et al., 2010, McKee et al., 2011; Gordon et al., 2015; Gruber et al., 2019b), the amount of C_{ant} stored in the AABWs may be very variable, which could bias the estimates of C_{ant} trends derived from data sets collected several years apart (e.g. Williams et al., 2015; Pardo et al., 2017; Murata et al., 2019).

In this context of potentially high variability in C_{ant} uptake at AABW formation sites, as well as in AABW export, circulation and mixing, we used repeated observations collected in the Indian sector of the Southern Ocean to explore the variability in C_{ant} and C_T in the AABW and evaluate their evolution over the last 40 years.

2 Studied area

2.1 AABW sampling during the last 40 years

Most of the data used in this study were obtained in the frame of the long-term observational project OISO (Ocean Indien Service d'Observations) conducted since 1998 onboard the R.S.V. Marion-Dufresne (IPEV/TAAF). During these cruises, several stations are visited, but only one station is sampled down to the bottom (4800 m) south of the Polar Front at 63.0° E and 56.5° S (hereafter noted OISO-ST11). This station is located in the Enderby Basin on the Western side of the Kerguelen Plateau (Fig. 1) and coincides with the station 75 of the INDIGO-3 cruise (1987). In our analysis, we also included data from the station 14 (deepest sample taken at 5109 m) of the INDIGO-1 cruise (1985) and the station 430 (deepest sample taken at 4710 m) of the GEOSECS cruise (1978) located near OISO-ST11 sampling site (405 km and 465 km away from it, respectively; Fig. 1). All the re-occupations used in this analysis are listed in Table 1. Since seasonal variations are only observed in the surface mixed layer (Metzl et al., 2006), we used the observations available for all seasons (Table 1).

Table 1

2.2 AABWs circulation in the Atlantic and Indian sectors of the Southern Ocean

The circulation in the SO is mainly governed by the Antarctic Circumpolar Current (ACC) that flows eastward, while the Coastal Antarctic Current (CAC) flows westward (Fig. 1). The ACC and the CAC influence the circulation of the entire water column, including the AABWs. The main AABW formation sites are the Weddell Sea, where Weddell Sea Deep Water and Weddell Sea Bottom Water are produced (WSDW and WSBW, respectively; Gordon, 2001; Gordon et al., 2010), the Ross Sea for the Ross Sea Bottom Water (RSBW; Gordon et al., 2009, 2015), the Adelie Land coast for the Adelie Land Bottom Water (ALBW; Williams et al., 2008, 2010) and the Cape Darnley Polynya for the Cape Darnley Bottom Water (CDBW; Ohshima et al., 2013). AABW formation has also been observed in the Prydz Bay (Yabuki et al., 2006; Rodehacke et al., 2007). There, three polynyas and two ice shelves have been identified as Prydz Bay Bottom Water (PBBW) production hotspots from seal tagging data (Williams et al., 2016). This PBBW flows out the Prydz Bay through the Prydz Channel and get mixed with the CDBW. The mix of CDBW and PBBW (hereafter called CDBW) represents a significant AABW export (13 % of all AABWs exports; Ohshima et al., 2013).

The largest bottom water source of the global ocean is the Weddell Sea (Gordon et al., 2001). The exported WSDW is a mixture of the WSBW and Warm Deep Water (WDW). The WDW is a slightly modified Low Circumpolar Deep Water (LCDW) by mixing with High Salinity Surface Water (HSSW) when the LCDW enters the Weddell

basin (see Fig. 2 in van Heuven et al., 2011). The WSDW mixes with the LCDW during its transit from the Weddell basin. A part of the WSDW deflecting southward with the ACC in the Enderby Basin reaches the north-western part of the Princess Elizabeth Trough (PET) region (area separating the Kerguelen Plateau from the Antarctic continent), where it mixes with other types of AABWs (Heywood et al., 1999; Orsi et al., 1999). The PET deepest point is 3750 m, deep enough to allow AABWs to flow between the Australian Antarctic Basin and the Enderby Basin (Heywood et al., 1999).

At the east of the PET, the CAC transports a mixture of RSBW and ALBW and accelerates northward along the eastern side of the Kerguelen Plateau (Mantyla and Reid, 1995; Fukamachi et al., 2010). Part of the ALBW-RSBW mixture also reaches the western side of the Kerguelen Plateau by the southern part of the PET (Heywood et al., 1999; Orsi et al., 1999; Van Wijk and Rintoul, 2014) and mixes with the CDBW. The mixture of CDBW and ALBW-RSBW either flows westward with the CAC and dilutes with the LCDW (Meijers et al., 2010) or flows northward (Ohshima et al., 2013) and mixes with the WSDW before reaching the location of our time-series station in the eastern Enderby Basin.

Figure 1

2.3 AABW definition

The distinction of water masses is usually performed according to neutral density (γ^n) layers. In the SO, LCDW and AABW properties are generally well defined in the range 28.15-28.27 kg.m^{-3} and 28.27-bottom, respectively (Orsi et al., 1999; Murata et al 2019). However, to interpret the long-term variability of the properties in the AABW core at our location, we prefer to adjust the AABW definition to a narrow (more homogeneous) layer that we call Lower Antarctic Bottom Water (LAABW), characterised by γ^n > 28.35 kg.m^{-3} (roughly ranging from 4200m to 4800m, see Fig. 3). This definition corresponds to the AABW characteristics observed at higher latitudes in the Indian SO sector (Roden et al., 2016). The layer above the LAABW is hereafter called Upper Antarctic Bottom Water (UAABW).

3 Material and methods

3.1 Validation of the data

For 1998-2004, the OISO data were quality controlled in CARINA (Lo Monaco et al., 2010) and for 2005 and 2009-2011 in GLODAPv2 (Key et al., 2015; Olsen et al., 2016, 2019). The 3 additional datasets from GEOSECS, INDIGO-1 and INDIGO-3 were first qualified in GLODAPv1 (Key et al., 2004) and used for the first C_{ant} estimates in the Indian Ocean (Sabine et al., 1999). The adjustments recommended for these historical datasets have been revisited in CARINA and GLODAPv2. In this paper we used the revised adjustments applied to the GLODAPv2 data product, with one exception for the total alkalinity (A_T) data from INDIGO-3 for which we applied an intermediate adjustment between the recommendation from GLODAPv1 (confirmed in CARINA) for no adjustment and the adjustment by -8 µmol.kg^{-1} applied to the GLODAPv2 data product (justification in Supp. Mat.).

For the recent OISO cruises conducted in 2012-2018 not yet included in the most recent GLODAPv2 product, we have proceeded to a data quality control in deep waters where C_{ant} concentrations are low and subject to very small changes from year to year (see Supp. Mat.).

3.2 Biogeochemical measurements

Measurement methods during OISO cruises were previously described (Jabaud-Jan et al., 2004; Metzl et al., 2006). In short, measurements were obtained using Conductivity-Temperature-Depth (CTD) casts fixed on a 24 bottles rosette equipped with 12 L General Oceanics Niskin bottles. Potential temperature (Θ) and salinity (S) measurements have an accuracy of 0.002 °C and 0.005 respectively. A_T and C_T were sampled in 500 mL glass bottles and poisoned with 100 µL of mercuric chloride saturated solution to halt biological activity. Discrete C_T and A_T samples were analyzed onboard by potentiometric titration derived from the method developed by Edmond (1970) using a closed cell. The repeatability for C_T and A_T varies from 1 to 3.5 µmol.kg^{-1} (depending on the cruise) and is determined by sample duplicates (in surface, at 1000 m and in bottom waters). The accuracy of C_T and A_T measurements was ensured by daily analyses of Certified Reference Materials (CRMs) provided by A.G. Dickson laboratory (Scripps Institute of Oceanography). Dissolved oxygen (O_2) concentration was determined by an oxygen sensor fixed on the rosette. These values were adjusted using measurements obtained by Winkler titrations using a potentiometric titration system (at least 12 measurements for each profile). The thiosulphate solution used for the Winkler titration was calibrated using iodate standard solution (provided by Ocean Scientific International Limited) to ensure the standard O_2 accuracy of 2 µmol.kg^{-1}. Nitrate (NO_3) and Silicate (Si) concentrations were measured onboard or onshore with an automatic colorimetric Technicon analyser following the methods described by Tréguer and Le Corre (1975) until 2008, and the revised protocol described by Aminot and Kérouel (2007) since 2009. Based on replicate measurements for deep samples we estimate an error of about 0.3 % for both nutrients. NO_3 data are not available for all the cruises used in this analysis. The mean NO_3 concentrations in the LAABW at OISO-ST11 is 32.8 ± 1.2 µmol.kg^{-1} while the average value derived from the GLODAP-v2 database in bottom waters south of 50°S in the South Indian Ocean is 32.4 ± 0.6 µmol.kg^{-1}. The lack of NO_3 data for few cruises has been palliated by considering a climatological value of 33 µmol.kg^{-1} with a limited impact on C_{ant} determined by the C° method (<2 µmol.kg^{-1} on estimates based on the differences observed between NO_3 measurements and the climatological value).

3.3 C_{ant} calculation using the TrOCA method

The TrOCA method was first presented by Touratier and Goyet (2004a, b) and revised by Touratier et al. (2007). Following the concept of the quasi-conservative tracer NO (Broecker, 1974), TrOCA is a tracer defined as a combination of O_2, C_T and A_T, following:

$$TrOCA = O_2 + a\left(C_T - \frac{1}{2}A_T\right), \quad (1)$$

where a is defined in Touratier et al. (2007) as combination of the Redfield equation coefficients for CO_2, O_2, HPO_4^{2-} and H^+. For more details about the definition and the calibration of this parameter, please refer to Touratier et al. (2007). The temporal change in TrOCA is independent of biological processes and can be attributed to anthropogenic carbon (Touratier and Goyet, 2004a). Therefore, C_{ant} can be directly calculated from the difference between TrOCA and its pre-industrial value TrOCA°:

$$C_{ant} = \frac{TrOCA - TrOCA^0}{a}, \quad (2)$$

where TrOCA° is evaluated as a function of θ and A_T (Eq. 3):

$$TrOCA^0 = e^{\left[b-(c).\Theta-\frac{d}{{A_T}^2}\right]}, \quad (3)$$

In these expressions, coefficients a, b, c and d were adjusted by Touratier et al. (2007) from free anthropogenic CO_2 deep waters using the tracers $\Delta^{14}C$ and CFC-11 from the GLODAPv1 database (Key et al., 2004). The final expression used to calculate C_{ant} is:

$$C_{ant} = \frac{O_2 + 1{,}279\left(C_T - \frac{1}{2}A_T\right) - e^{\left[7{,}511 - (1{,}087.10^{-2}).\Theta - \frac{7{,}81.10^5}{{A_T}^2}\right]}}{1{,}279}, \quad (4)$$

The consideration of the errors on the different parameters involved in the TrOCA method results in an uncertainty of ±6.25 µmol.kg^{-1} (mostly due to the parameter a, leading to ±3.31 µmol.kg^{-1}). As this error is relatively large compared to the expected Cant concentrations in deep and bottom SO waters (Pardo et al., 2014) we will compare the TrOCA results using another indirect method to interpret C_{ant} changes over 40 years.

3.4 C_{ant} calculation using the preformed inorganic carbon (C^0) method

To support the C_{ant} trend determined with the TrOCA method, C_{ant} was also estimated using a back-calculation approach noted C^0 (Brewer, 1978; Chen and Millero, 1979), previously adapted for C_{ant} estimates along the WOCE-I6 section between South Africa and Antarctica (Lo Monaco et al., 2005a). This method consists in the correction of the measured C_T for the biological contribution (C_{bio}) and the preindustrial preformed C_T (C^0_{PI}):

$$C_{ant} = C_T - C_{bio} - C^0_{PI}, \quad (5)$$

C_{bio} (Eq. 6) depends on carbonate dissolution and organic matter remineralization, taking account of the corrected C/O_2 ratio from Kortzinger et al. (2001):

$$C_{bio} = 0.5\Delta A_T - (C/O_2 + 0.5N/O_2)\Delta O_2, \quad (6)$$

Where C/O_2 = 106/138 and N/O_2 = 16/138. ΔA_T and ΔO_2 are the difference between the measured values (A_T and O_2) and the preformed values (A_T^0 and O_2^0). A_T^0 (Eq. 7) has been computed by Lo Monaco et al. (2005a) as a function of Θ, S and the conservative tracer PO:

$$A_T^0 = 0.0685PO + 59.79S - 1.45\Theta + 217.1, \quad (7)$$

PO (Eq. 8) has been defined by Broecker (1974) and depends on the equilibrium of O_2 with phosphate (PO_4). When PO_4 data are not available, nitrate (NO_3) can be used instead as follows (the N/P ratio of 16 is from Anderson and Sarmiento, 1994):

$$PO = O_2 + 170PO_4 = O_2 + (170/16)NO_3, \quad (8)$$

To determine O_2^0, it is assumed that the surface water is in full equilibrium with the atmosphere ($O_2^0 = O_{2,sat}$; Benson and Krause, 1980) and that after subduction O_2 in a given water mass is only impacted by the biological activity (Weiss, 1970). A correction of O_2^0 has been proposed by Lo Monaco et al. (2005a) to take account of the undersaturation of O_2 due to sea-ice cover at high latitudes. O_2^0 is, therefore, corrected by assuming a mean mixing ratio of the ice-covered surface waters k=50 % (Lo Monaco et al., 2005a), and a mean value for O_2 undersaturation in ice-covered surface waters α = 12 % (Anderson et al., 1991) according to Eq. 9:

$$\Delta O_2 = (1 - \alpha k)O_{2,sat} - O_2 = AOU, \quad (9)$$

C^0_{PI} in equation 5 is a function of the current preformed C_T (C^0_{obs}) and a reference water term (Eq. 10):

$$C^0_{PI} = C^0_{obs} + [C_T - C_{bio} - C^0_{obs}]_{REF}, \quad (10)$$

$C_{0,obs}$ has been computed similarly as A_T^0 (Eq. 11):

$$C^0_{obs} = -0.0439PO + 42.79S - 12.02\Theta + 739.8, \quad (11)$$

Where the reference water term is a constant for a given time of observation, corresponding to the time when C^0_{obs} is parameterized. In this paper, we used the parameterization given by Lo Monaco et al., (2005a) and their estimated value for the reference term of 51 µmol.kg^{-1}. This number has been computed using an optimum multiparametric (OMP) model to estimate the mixing ratio of the North Atlantic deep water in the SO (used as reference water, i.e. old water mass where $C_{ant} = 0$). For more details about the C^0 method, which has a final error of ± 6 µmol.kg^{-1}, please see Lo Monaco et al. (2005a).

4 Results

The vertical distribution of hydrological and biogeochemical properties observed in deep and bottom waters and their evolution over the last 40 years are displayed in Fig 2. The LCDW layer (γ^n = 28.15-28.27 kg.m^{-3}) is characterized by minimum O_2 concentrations (Fig. 2c), higher C_T (Fig. 2b) and lower C_{ant} concentrations than in the AABW (Fig. 2a). C_{ant} concentrations were not significant in the LCDW until the end of the 1990s (<6 µmol.kg^{-1}), then our data show an increase in C_{ant} between the two 1998 reoccupations, followed by relatively constant C_{ant} concentrations (10±3 µmol.kg^{-1}). In the LAABW (γ^n > 28.35 kg.m^{-3}), well identified by low Θ, low S and high O_2, C_{ant} concentrations are higher than in the overlying UAABW and LCDW (Fig. 2a). The evolutions of the mean properties in the LAABW over 40 years are shown in Fig. 3. In this layer, C_{ant} concentrations increased from 5±4 µmol.kg^{-1} in 1978 and 7±4 µmol.kg^{-1} in the mid-1980s to 13±2 µmol.kg^{-1} at the end of the 1990s and up to 19±2 µmol.kg^{-1} in 2004 (Fig. 3a). Figure 3a also shows a very good agreement between the TrOCA method and the C^0 method for both the magnitude and variability of C_{ant} in the LAABW. Our results show a mean C_{ant} trend in the LAABW of +1.4 µmol.kg^{-1}.decade^{-1} over the full period and a maximum trend of the order of +5.2 µmol.kg^{-1}.decade^{-1} over 1987-2004 (Table 2). These trends are lower than the theoretical trend expected from the increase in atmospheric CO_2. Indeed, assuming that the surface ocean fCO_2 follows the atmospheric growth rate (+1.8 µatm.year^{-1} over 1978-2018), the theoretical C_{ant} trend at the AABW formation sites would be of the order of +8 µmol.kg^{-1}.decade^{-1}. The observed slow C_{ant} trends can be partly explained by the transit time for AABW to reach our study site and the mixing of AABWs with older LCDW that contain less C_{ant} over their transit (Fig. 2a).

Figure 2

Over the full period, C_T increased by 2.0±0.5 µmol.kg^{-1}.decade^{-1}, mostly due to the accumulation of C_{ant} (Table 2). Our data also show a significant decrease in O_2 concentrations by 0.8±0.4 µmol.kg^{-1}.decade^{-1} over the 40-years period (Fig. 3c, Table 2) that could be caused by reduced ventilation, as suggested by Schmidtko et al. (2017) who observed significant O_2 loss in the global ocean. In the deep Indian SO sector, these authors found a trend approaching -1 µmol.kg^{-1}.decade^{-1} over 50 years (1960-2010), which is consistent with our data. We did not detect any significant trend in A_T, Θ and S over the full period, but on shorter periods our data show a significant decrease in A_T. The low A_T values observed over 2000-2004 (Fig. 3d) could suggest reduced calcification in the upper ocean leading to less sinking of calcium carbonate tests and a decrease in A_T in deep and bottom waters over this period (Fig. 2d). For this period the increase in C_T was lower than the accumulation of C_{ant}, but such feature is disputable in view of the uncertainty on the C_{ant} calculation. This event is followed by an increase in the 'natural' component of C_T (C_{nat}, calculated as the difference between C_T and C_{ant}) since 2004 associated to a decrease in O_2 and no increase in C_{ant} (Table 2). These trends were not associated with a significant trend in θ or S (Fig. 3e,f, Table 2). The increase in C_{nat} is thus unlikely originating from increased mixing with LCDW during bottom waters

transport, confirming that our LAABW definition exclude mixing with the LCDW. Enhanced organic matter remineralization is also unlikely since NO_3 did not show any significant trend (Table 2).

Table 2

Figure 3

Importantly, our data show substantial interannual variations in LAABW properties, which could significantly impact the trends estimated from limited reoccupations (e.g. Williams et al., 2015; Pardo et al., 2017; Murata et al., 2019). For example, we found relatively higher C_{ant} concentrations in 1985 (10 µmol.kg^{-1}) compared to 1978 (5 µmol.kg^{-1}) and 1987 (7 µmol.kg^{-1}). This is linked to a signal of low S in 1985 (Fig. 3f) that could be due to a larger contribution of fresher waters such as the WSDW or CDBW. This could also be related to the different sampling locations. Over the last decade (2009-2018), our data show large and rapid changes in S that are partly reflected on C_T and O_2, and that could explain the relatively low C_{ant} concentrations observed over this period. Indeed, the S maximum observed in 2012 (correlated to higher θ) is associated with a marked C_T minimum (surprisingly almost as low as in 1987), as well as low A_T (hence low C_{Tnat}), and low NO_3 concentrations. Since these anomalies were associated with a decrease in C_{ant} concentrations, one may argue for an increased contribution of bottom waters ventilated far away from our study site. A few years later our data show a S minimum (correlated to lower θ), associated with a rapid increase in C_T and a rapid decrease in O_2 between 2013 and 2016, suggesting the contribution of a closer AABW type such as the CDBW. The freshening of -0.006 decade^{-1} in S between 2004 and 2018 that we observed on the western side of the Kerguelen Plateau was also observed on the eastern side of the Plateau by Menezes et al. (2017) over a similar period. In this region, Menezes et al. (2017) evaluated a change in S by about -0.008 decade^{-1} from 2007 to 2016 (against -0.002 decade^{-1} between 1994 and 2007), suggesting an acceleration of the AABW freshening in recent years. However, they also reported a warming by +0.06 °C.decade^{-1}, while we observed cooler temperature in 2016-2018. This suggests that we sampled a different mixture of AABWs.

Figure 4

5 Discussion

5.1 LAABW composition at OISO-ST11

At each formation site, AABWs experienced significant temporal property changes, mostly recognized at decadal scale (e.g. freshening in the South Indian Ocean, Menezes et al., 2017) with potential impact on carbon uptake and C_{ant} concentrations during AABW formation (Shadwick et al., 2013). The Θ-S diagram constructed from yearly averaged data in bottom waters (Fig. 4) shows that the LAABW at OISO-ST11 is a complex mixture of WSDW, CDBW, RSBW and ALBW. The coldest type of LAABW was observed at the GEOSECS station at 60° S (-0.56 °C), while the warmer type of LAABW observed at the INDIGO-1 station at 53° S (-0.44 °C). These extreme Θ values could be a natural feature or may be related to specific sampling. For the other cruises, Θ in LAABW ranges from -0.51 to -0.45 °C with no clear indication on the specific AABW origin. The S range observed in the bottom waters at OISO-ST11 (34.65-34.67) illustrates either changes in mixing with various AABW sources or temporal variations at the formation site. Given the knowledge of deep and bottom waters circulation and characteristics (Fig. 1 and 4) and the significant C_{ant} concentrations that we calculated in the LAABW (Fig. 3a), the main contribution at our location is likely the younger and colder CDBW for which relatively high C_{ant} concentrations

have been recently documented (Roden et al., 2016). From its formation region, the CDBW can either flow westward with the CAC or flow northward in the Enderby Basin (Ohshima et al., 2013, Fig. 1). In the CAC branch, the CDBW mixes with the LCDW along the Antarctic shelf and the continental slope between 80° E and 30° E (Meijers et al., 2010; Roden et al., 2016). On the western side of the Kerguelen Plateau, CDBW also mixes with RSBW and ALBW (Orsi et al., 1999; Van Wijk and Rintoul, 2014). In this context, the Cant concentrations observed in the bottom layer at OISO-ST11 are probably not linked to one single AABW source, but are likely a complex interplay of AABWs from different sources with different biogeochemical properties.

5.2 C_{ant} concentrations

In order to compare our C_{ant} estimates with other studies, we separated the 40-years time-series into 3 periods: the first period (1978-1987) corresponds to historical data when C_{ant} is expected to be low; the second period (1998-2004) starts when the first OISO cruise was conducted (and using CRMs for A_T and C_T measurements) and lasts when C_{ant} concentrations in the LAABW are maximum (Fig. 3a); the third period consists in the observations performed in late 2009 to 2018 when the observed variations are relatively large for S and small for C_{ant}. The mean C_{ant} concentrations for each period are 7, 14 and 13 µmol.kg^{-1}, respectively, which is consistent with the results from other studies (Table 3). The C_{ant} values for 1978-1987 can hardly be compared to other studies because very few observations were conducted in the 1980s in the SO Indian sector (Sabine et al., 1999) and because of potential biases for historical data despite their careful qualification in GLODAP and CARINA (Key et al., 2004; Lo Monaco et al., 2010; Olsen et al., 2016). In addition, the different methods used to estimate C_{ant} can lead to different results, especially in deep and bottom waters of the SO (Vázquez-Rodríguez et al., 2009). Overall, Table 3 confirms that C_{ant} concentrations were low in the 1970s and 1980s, and reached values of the order of 10 µmol.kg^{-1} in the 1990s, a signal not clearly captured in global data-based estimates (Gruber, 1998; Sabine et al., 2004; Waugh et al., 2006; Khatiwala et al., 2013).

The observations presented in this analysis, although regional, offer a complement to recent estimates of C_{ant} changes evaluated between 1994 and 2007 in the top 3000 m for the global ocean (Gruber et al., 2019a). In the Enderby Basin at the horizon 2000-3000 m, the accumulation of C_{ant} from 1994 to 2007 is not uniform and ranges between 0 and 8 µmol.kg^{-1} (Gruber et al., 2019a). At our station, in the LCDW (2000-3000m) the C_{ant} concentrations were not significant in 1978-1987 (-2 to 5 µmol.kg^{-1}) but increase to an average of 9±3 µmol.kg^{-1} in 1998-2018 (Fig. 2a), probably due to mixing with AABWs that contain more C_{ant}. Interestingly, this value is close but in the high range of the C_{ant} accumulation estimated from 1994 to 2007 in deep waters of the south Indian Ocean (Gruber et al., 2019a).

Not surprisingly, high C_{ant} concentrations are detected in the AABW formation regions (Table 3). The highest C_{ant} concentrations in bottom waters (up to 30 µmol.kg^{-1}) were observed in the ventilated shelf waters in the Ross Sea (Sandrini et al., 2007). In the Adélie and Mertz Polynya regions, Shadwick et al. (2014) observed high C_{ant} concentrations in the subsurface shelf waters (40-44 µmol.kg^{-1}) but lower values in the ALBW (15 µmol.kg^{-1}) due to mixing with older LCDW. In WSBW, all C_{ant} concentrations estimated from observations between 1996 and 2005 and with the TrOCA method (Table 3) lead to about the same values ranging between 13 and 16 µmol.kg^{-1} (Lo Monaco et al., 2005b; van Heuven et al., 2011). In bottom waters formed near the Cape Darnley (CDBW), Roden et al. (2016) estimated high C_{ant} concentrations in bottom waters (25 µmol.kg^{-1}) resulting from the shelf

waters that contain very high amounts of C_{ant} (50 µmol.kg^{-1}). The comparison with other studies confirms that far from the AABW formation sites, contemporary C_{ant} concentrations are not exceeding 16 µmol.kg^{-1} on average. Table 3.

5.3 C_{ant} trends and variability

Comparison of long-term C_{ant} trends in deep and bottom waters of the SO is limited to very few regions where repeated observations are available. To our knowledge, only 3 other studies evaluated the long-term C_{ant} trends in the SO based on more than 5 reoccupations: in the South-western Atlantic (Rios et al., 2012) and in the Weddell Gyre along the Prime meridian section (van Heuven et al., 2011, 2014). Temporal changes of C_T and C_{ant} have also been investigated in other SO regions, but limited to 2 to 4 reoccupations (Williams et al., 2015; Pardo et al., 2017; Murata et al., 2019). Given the C_{ant} variability depicted at our location (Fig. 3a), different trends can be deduced from limited reoccupations. As an example, Murata et al., (2019) evaluated the change in C_{ant} from data collected 17 years apart (1994–1996 and 2012–2013) along a transect around 62° S and found a small increase at our location (< 5 µmol.kg^{-1} around 60° E). This result appears very sensitive to the time of the observation given that we found a minimum in C_{ant} concentrations between 2011 and 2014 (Fig. 3a) associated with a marked C_T minimum (Fig. 3b). In addition, our results show that the detection of C_{ant} trends appears very sensitive to the time period considered (Table 2). As an extreme case, the C_{ant} trend calculated for the period 1987-2004 is +5.2 µmol.kg^{-1}.decade^{-1} (relatively close to the theoretical C_{ant} trend of +8 µmol.kg^{-1}.decade^{-1}), but it reverses to -3.5 µmol.kg^{-1}.decade^{-1} for the period 2004-2018.

The long-term C_T trend that we estimated in the LAABW in the eastern Enderby Basin (2.0±0.5 µmol.kg^{-1}.decade^{-1}) is slightly faster than the C_T trends estimated in the WSBW in the Weddell Gyre: +1.2±0.5 µmol.kg^{-1}.decade^{-1} over the period 1973-2011 and +1.6±1.4 µmol.kg^{-1}.decade^{-1} when restricted to 1996-2011 (van Heuven et al., 2014). Along the SR03 line (south of Tasmania) reoccupied in 1995, 2001, 2008 and 2011, Pardo et al. (2017) calculated a C_T trend of +2.4±0.2 µmol.kg^{-1}.decade^{-1} in the AABW, composed of ALBW and RSBW in this sector. This is higher than the C_T trends found at our location and in the Weddell Gyre, but surprisingly, this was not associated with a significant increase in C_{ant}. The C_T trend in AABW along the SR03 section was likely due to the intrusion of old and C_T-rich waters also revealed by an increase in Si concentrations during 1995-2011 (Pardo et al., 2017). This is a clear example of decoupling between C_T and C_{ant} trends in deep and bottom waters as observed at our location in the last decade (Table 2). For C_{ant}, our 40-years trend estimate (1.4±0.5 µmol.kg^{-1}.decade^{-1}) appears close to the trend reported by Rios et al. (2012) in the south-western Atlantic AABW from 6 reoccupations between 1972 and 2003 (+1.5 µmol.kg^{-1}.decade^{-1}). However, if we limit our result to the period 1978-2002 or 1978-2004 (about the same period as in Rios et al., 2012), our trend is much larger (+3-4 µmol.kg^{-1}.decade^{-1}).

At our location, the C_{ant} trend over 40 years (+1.4±0.5 µmol.kg^{-1}.decade^{-1}) explains most of the observed C_T increase (+2.0±0.5 µmol.kg^{-1}.decade^{-1}). The residual of +0.4 µmol.kg^{-1}.decade^{-1} reflects changes in natural processes affecting the carbon content (different AABW sources, ventilation, mixing with deep waters, remineralization or carbonates dissolution). Although this is a weak signal, the natural C_T change (C_{nat}) mirrors the observed decrease in O_2 by -0.8±0.4 µmol.kg^{-1}.decade^{-1}. This O_2 decrease detected in the Enderby Basin appears to be a real feature that was documented at large scale for 1960-2010 in deep SO basins (Schmidtko et al. 2017), suggesting that the changes observed at 56.5°S/63°E are related to large-scale processes, possibly due to a decrease in AABW formation (Purkey and Johnson, 2012).

5.4 Recent C_{ant} stability

Although most studies suggest a gradual accumulation of C_{ant} in the AABW, our time-series highlights significant multi-annual changes, in particular over the last decade when C_{ant} concentrations were as low as around the year 2000 (Fig. 3a) and decoupled from the increase in C_T (Fig. 3b). This result is difficult to interpret because at our location, away from AABW sources (Fig. 1), the temporal variability observed in the LAABW layer can result from many remote processes occurring at the AABW formation sites (such as wind forcing, ventilation, sea-ice melting, thermodynamic, biological activity and air-sea exchanges). Additionally, internal processes during the transport of AABWs (such as organic matter remineralization, carbonate dissolution and mixing with surrounding waters) must also be taken into account. The apparent steady C_{ant} feature suggests that AABWs found at our location has stored less C_{ant} in recent years. This might be linked to reduced CO_2 uptake in the AABW formation regions, as recognized at large-scale in the SO from the late 1980s to 2001 (Le Quéré et al., 2007; Metzl, 2009; Lenton et al., 2012; Landschützer et al., 2015). This large-scale response in the SO during a positive trend in the Southern Annular Mode (SAM) is mainly associated to stronger winds driven by accelerating greenhouse gas emissions and stratospheric ozone depletion, leading to warming and freshening in the SO (Swart et al., 2018), change in the ventilation of the C_T-rich deep waters and reduced CO_2 uptake (Lenton et al., 2009). The reconstructed pCO_2 fields by Landschützer et al. (2015) suggest that the reduced CO_2 sink in the 1990s is identified at high latitudes in the SO (see Fig. 2a and S9 in Landschützer et al., 2015). However, as opposed to the circumpolar open ocean zone (e.g. Metzl, 2009; Takahashi et al., 2009, 2012; Munro et al., 2015; Fay et al., 2018), the long-term trend of surface fCO_2 and carbon uptake deduced from direct observations are not clearly identified in the seasonal ice zone (SIZ) and shelves around Antarctica, and thus in the AABW formation regions of interest to interpret our results (Laruelle et al., 2018). There, surface fCO_2 data are sparse, especially before 1990, and cruises were mainly conducted in austral summer when the spatio-temporal fCO_2 variability is very large and driven by multiple processes at regional or small scales, such as primary production, sea-ice formation and retreat, and water circulation and mixing. This leads to various estimates of the air-sea CO_2 fluxes around Antarctica depending on the region and period and large uncertainty when attempting to detect long-term trends (Gregor et al., 2018).

In particular, in polynyas and AABW formation regions where fCO_2 is low and where katabatic winds prevail, very strong instantaneous CO_2 sink can occur at the local scale (up to -250 mmol $C.m^{-2}.d^{-1}$ in Terra Nova Bay in the Ross Sea according to De Jong and Dunbar, 2017). In the Prydz Bay region where CDBW is formed, recent studies show that surface fCO_2 in austral summer vary over a very large range (150-450 µatm), with the lowest fCO_2 observed in the shelf region generating very strong local CO_2 sink (-221 mmol $C.m^{-2}.d^{-1}$; Roden et al. 2016). The carbon uptake was particularly enhanced near Cape Darnley and coincided with the highest C_{ant} concentrations that Roden et al. (2016) estimated in the dense shelf waters that subduct to form AABW. In the Prydz Bay coastal region, surface fCO_2 values in 1993-1995 were as low as 100 µatm (Gibson and Trull, 1999) leading to a strong local CO_2 uptake of -30 mmol $C.m^{-2}.d^{-1}$ in summer. In addition, Roden et al. (2013) found a large C_T increase over 16 years (+34 $\mu mol.kg^{-1}$) in the Prydz Bay, which is much higher than the anthropogenic signal alone (+12 $\mu mol.kg^{-1}$) and likely explained by changes in primary production that would have been stronger in 1994. To our knowledge, this is the only direct observation of decadal C_T change in surface waters in a region of AABW formation (here the Prydz Bay) and it highlights the difficulty not only to evaluate the C_T and C_{ant} long-term trends in these regions but also to separate natural and anthropogenic signals when this water reaches the deep ocean. We attempted to detect long-term changes in CO_2 uptake in this region using the qualified fCO_2 data available in the

SOCAT database (Bakker et al., 2016), but our estimates (not shown) were highly uncertain due to very large spatial and temporal variability. To conclude, all previous studies conducted near or in AABW formation sites clearly reveal that these regions are potentially strong carbon sinks, but how the sink changed over the last decades is not yet evaluated, and thus we are not able to certify that the recent C_{ant} stability that we observed in the LAABW at our location is directly linked to the weakening of the carbon sink that was recognized at large-scale in the SO from the 1980s to mid-2000s (Le Quéré et al., 2007; Landschützer et al., 2015).

Changes in the accumulation of C_{ant} in AABW could also be directly related to changes in physical processes occurring in AABW formation regions. Decadal decreasing of sea-ice production and melting of sea-ice have been documented in several regions including Cape Darnley polynyas (Tamura et al., 2016; Williams et al., 2016). The consequent changes in Antarctic surface waters properties are transmitted into the deep ocean, notably the well-recognized freshening of AABWs over the last decades (Rintoul, 2007). The warming of bottom waters was also documented in the Enderby basin (Couldrey et al., 2013) as well as at a larger scale in all deep SO basins (Purkey and Johnson, 2010; Desbruyères et al., 2016). Associated to a decrease in AABW formation in the 1990s (Purkey and Johnson, 2012), these physical changes could explain the recent stability of C_{ant} concentrations in AABW observed at our location. As AABWs from different sources spread and mix with C_T-rich deep waters before reaching our location (Fig. 1), less AABW formation and export would result in an increase in C_T (increase in C_{nat}) not associated with an increase in C_{ant}, and a decrease in O_2 (as observed in recent years in Fig. 3a,b,c). Finally, it is also possible that the LAABW observed in recent years at our location is the result of a larger contribution of older RSBW, ALBW or even WSBW that have lower C_{ant} and O_2 concentrations compared to CDBW formed at Cape Darnley and Prydz Bay.

6 Conclusion

The distribution and evolution of C_{ant} in the bottom layer of the SO are related to complex interactions between climatic forcing, air-sea CO_2 exchange at formation sites, as well as biological and physical processes during AABWs circulation. The dataset that we collected regularly in the Enderby basin over the last 20 years (1998-2018) in the frame of the OISO project, together with historical observations obtained in 1978, 1985 and 1987 (GEOSECS and INDIGO cruises), allows the investigation of C_{ant} changes in AABW over 40 years in this region. The focus on the AABW variability is made by defining a Low Antarctic Bottom Water (LAABW) as described in the Section 2.3. Our results suggest that the accumulation of C_{ant} explains most, but not all, of the observed increase in C_T. We also detected a decrease in O_2 that is consistent with the large-scale signal reported by Schmidtko et al. (2017), possibly due to a decrease in AABWs formation (Purkey and Johnson, 2012). Our data further indicate rapid anomalies in some periods suggesting that for decadal to long-term estimates care have to be taken when analyzing the change in C_{ant} from data sets collected 10 or 20 years apart (e.g. Williams et al., 2015; Murata et al., 2019). Our results also show different C_{ant} trends on short periods, with a maximum increase of 6.5 $\mu mol.kg^{-1}.decade^{-1}$ between 1987 and 2004 and an apparent stability in the last 20 years (despite an increase in C_T). This suggests that AABWs have stored less C_{ant} in the last decade, but our understanding of the processes that explain this signal is not clear. This might be the result of the reduced CO_2 uptake in the SO in the 1990s (Le Quéré et al., 2007; Landschützer et al., 2015), but this is not yet verified from direct C_T or fCO_2 observations in AABW formation regions due to the lack of winter data and very large variability during summer. This calls for more data

collection and investigations in these regions. The apparent stability of C_{ant} in the LAABW since 1998 could also be directly linked to a decrease in AABWs formation in the 1990s (Purkey and Johnson, 2012) or a change in the contributions of AABWs from different sources, especially in the Prydz Bay region (Williams et al., 2016). In these scenarios, an increased contribution of C_T-rich and O_2-poor older LCDW along AABWs transit would also explain the decoupling between C_{ant} and C_T (increase in C_{nat}) and decrease in O_2 concentrations observed in recent years, even if we tried to isolate this specific feature in our data selection. The decoupling between C_{ant} and C_T is not a unique feature, as it was also reported along the SR03 section between Tasmania and Antarctica, most probably due to advection of C_T-rich waters (Pardo et al., 2017). This highlights the importance of the ocean circulation in influencing the temporal C_T and C_{ant} inventories changes (De Vries et al., 2017) and the need to better separate anthropogenic and natural variability based on time-series observations.

The evaluation and understanding of decadal C_{ant} changes in deep and bottom ocean waters are still challenging, as the C_{ant} concentrations remain low compared to C_T measurements accuracy (at best ±2 µmol.kg^{-1}, Bockmon and Dickson, 2015) and uncertainties of data-based methods (±6 µmol.kg^{-1}). Long-term repeated and qualified observations (at least 30 years) are needed to accurately detect and separate the anthropogenic signal from the internal ocean variability; we thus only start to document these trends that should now help to identify shortcomings in models regarding the carbon storage in the deep SO (e.g. Frölicher et al., 2014). As changes in the SO (including warming, freshening, oxygenation/deoxygenation, CO_2 and acidification) are expected to accelerate in the future in response to anthropogenic forcing and climate change (e.g. Heuzé et al., 2014; Hauck et al., 2015; Ito et al., 2015, Yamamoto et al., 2015), it is important to maintain time-series observations to complement the GO-SHIP strategy, and to occupy more regularly other sectors of the SO (Rintoul et al., 2012). In this context, we hope to maintain our observations in the Southern Indian Ocean in the next decade, and with ongoing synthetic products activities such as GLODAPv2 (Olsen et al., 2016, 2019), SOCAT (Bakker et al., 2016) and more recently the SOCCOM project (Williams et al., 2018), to offer a solid database to validate ocean biogeochemical models and coupled climate/carbon models (Russell et al. 2018), and ultimately reduce uncertainties in future climate projections.

Data availability

GEOSECS, INDIGO and OISO 1998-2011 data are publicly available at the Ocean Carbon Data System (OCADS; https://www.nodc.noaa.gov/ocads/oceans/GLODAPv2_2019). OISO original data are available at: www.nodc.noaa.gov/ocads/oceans/RepeatSections/clivar_oiso.html. OISO 2012-2018 will be available in GLODAPv2_2021.

Author contributions

LM, CLM, NM, JF and CM performed the sampling and carried out the measurements of the OISO data. LM prepared the manuscript with contributions from CLM and NM.

Competing interests

The authors declare that they have no conflict of interest.

Acknowledgements

We thank the captains and crew of the R.S.V. Marion Dufresne and the staff at the French Polar Institute (IPEV) for their important contribution to the success of the cruises since 1998. We are also very grateful to all colleagues, students and technicians who helped to obtain the data. We extend our gratitude to P. C. Pardo, S. R. Rintoul and B. Legresy for the discussions during the preparation of the manuscript and to M. K. Shipton for the valuable comments. We thank two anonymous reviewers for their comments and constructive suggestions that helped improve the manuscript. The OISO program was and is supported by the French institutes INSU, IPEV and OSU Ecce-Terra and the French program SOERE/Great-Gases. Support from the European Integrated Projects CARBOOCEAN (511176) and CARBOCHANGE (264879) is also acknowledged.

References

Álvarez, M., Lo Monaco, C., Tanhua, T., Yool, A., Oschlies, A., Bullister, J. L., Goyet, C., Metzl, N., Touratier, F., McDonagh, E. and Bryden, H. L.: Estimating the storage of anthropogenic carbon in the subtropical Indian Ocean: a comparison of five different approaches, Biogeosciences, 6(4), 681–703, doi:10/cjvsn6, 2009.

Aminot A. and Kérouel R.: Dosage automatique des nutriments dans les eaux marines : méthodes en flux continu. Ed. Ifremer, Méthodes d'analyse en milieu marin 188 pp., 2007.

Anderson, L. A. and Sarmiento, J. L.: Redfield ratios of remineralization determined by nutrient data analysis, Glob. Biogeochem. Cycle, 8(1), 65–80, doi:10/bwbg6b, 1994.

Anderson, L. G., Holby, O., Lindegren, R. and Ohlson, M.: The transport of anthropogenic carbon dioxide into the Weddell Sea, J. Geophys. Res. Oceans, 96(C9), 16679–16687, doi:10/bs6f2j, 1991.

de Baar, H. J. W.: Options for enhancing the storage of carbon dioxide in the oceans: A review, Energy Convers. Manag., 33(5), 635–642, doi:10/cqf9gd, 1992.

Bakker, D. C. E., Pfeil, B., Landa, C. S., Metzl, N., O'Brien, K. M., Olsen, A., Smith, K., Cosca, C., Harasawa, S., Jones, S. D., Nakaoka, S., Nojiri, Y., Schuster, U., Steinhoff, T., Sweeney, C., Takahashi, T., Tilbrook, B., Wada, C., Wanninkhof, R., Alin, S. R., Balestrini, C. F., Barbero, L., Bates, N. R., Bianchi, A. A., Bonou, F., Boutin, J., Bozec, Y., Burger, E. F., Cai, W.-J., Castle, R. D., Chen, L., Chierici, M., Currie, K., Evans, W., Featherstone, C., Feely, R. A., Fransson, A., Goyet, C., Greenwood, N., Gregor, L., Hankin, S., Hardman-Mountford, N. J., Harlay, J., Hauck, J., Hoppema, M., Humphreys, M. P., Hunt, C. W., Huss, B., Ibánhez, J. S. P., Johannessen, T., Keeling, R., Kitidis, V., Körtzinger, A., Kozyr, A., Krasakopoulou, E., Kuwata, A., Landschützer, P., Lauvset, S. K., Lefèvre, N., Lo Monaco, C., Manke, A., Mathis, J. T., Merlivat, L., Millero, F. J., Monteiro, P. M. S., Munro, D. R., Murata, A., Newberger, T., Omar, A. M., Ono, T., Paterson, K., Pearce, D., Pierrot, D., Robbins, L. L., Saito, S., Salisbury, J., Schlitzer, R., Schneider, B., Schweitzer, R., Sieger, R., Skjelvan, I., Sullivan, K. F., Sutherland, S. C., Sutton, A. J., Tadokoro, K., Telszewski, M., Tuma, M., Heuven, S. M. A. C. van, Vandemark, D., Ward, B., Watson, A. J. and Xu, S.: A multi-decade record of high-quality fCO2 data in version 3 of the Surface Ocean CO2 Atlas (SOCAT), Earth Syst. Sci. Data, 8(2), 383–413, doi:10/f3sgd6, 2016.

524 Benson, B. B. and Krause, D.: The concentration and isotopic fractionation of gases dissolved in freshwater in
525 equilibrium with the atmosphere. 1. Oxygen: Oxygen in freshwater, Limnol. Oceanogr., 25(4), 662–671,
526 doi:10/d5cgt8, 1980.

527 Bockmon, E. E. and Dickson, A. G.: An inter-laboratory comparison assessing the quality of seawater carbon
528 dioxide measurements, Mar. Chem., 171, 36–43, doi:10/f66mfw, 2015.

529 Brewer, P. G.: Direct observation of the oceanic CO2 increase, Geophys. Res. Lett., 5(12), 997–1000,
530 doi:10/d4tk22, 1978.

531 Broecker, W. S.: "NO", a conservative water-mass tracer, Earth Planet. Sci. Lett., 23(1), 100–107, doi:10/frw2mm,
532 1974.

533 Carmack, E. C. and Foster, T. D.: Circulation and distribution of oceanographic properties near the Filchner Ice
534 Shelf, Deep-Sea Res. Oceanogr. Abstr., 22(2), 77–90, doi:10/cm46nh, 1975.

535 Chen, C.-T. A.: On the distribution of anthropogenic CO2 in the Atlantic and Southern oceans, Deep Sea Res. Part
536 A Oceanogr. Res. Pap., 29(5), 563–580, doi:10/cfgbkb, 1982.

537 Chen, C.-T. A.: The oceanic anthropogenic CO2 sink, Chemosphere, 27(6), 1041–1064, doi:10/fndnpx, 1993.

538 Chen, C.-T. A. and Millero, F. J.: Gradual increase of oceanic CO2, Nature, 277, 205, doi:10/cwp6k7, 1979.

539 DeJong, H. B. and Dunbar, R. B.: Air-Sea CO2 Exchange in the Ross Sea, Antarctica, J. Geophys. Res. Oceans,
540 122(10), 8167–8181, doi:10/gcmcs3, 2017.

541 Desbruyères, D. G., Purkey, S. G., McDonagh, E. L., Johnson, G. C. and King, B. A.: Deep and abyssal ocean
542 warming from 35 years of repeat hydrography, Geophys. Res. Lett., 43(19), 10,356-10,365, doi:10/f89qrt, 2016.

543 DeVries, T., Holzer, M. and Primeau, F.: Recent increase in oceanic carbon uptake driven by weaker upper-ocean
544 overturning, Nature, 542(7640), 215–218, doi:10/f9pm4w, 2017.

545 Edmond, J. M.: High precision determination of titration alkalinity and total carbon dioxide content of sea water
546 by potentiometric titration, Deep Sea Res. and Oceanogr. Abs., 17(4), 737–750, doi:10/d496rw, 1970.

547 Fahrbach, E., Rohardt, G., Schröder, M. and Strass, V.: Transport and structure of the Weddell Gyre, Ann.
548 Geophys., 12(9), 840–855, doi:10/fxg7nh, 1994.

549 Fay, A. R., Lovenduski, N. S., McKinley, G. A., Munro, D. R., Sweeney, C., Gray, A. R., Landschuetzer, P.,
550 Stephens, B. B., Takahashi, T. and Williams, N.: Utilizing the Drake Passage Time-series to understand variability
551 and change in subpolar Southern Ocean pCO(2), Biogeosciences, 15(12), 3841–3855, doi:10/gdsttn, 2018.

552 Frölicher, T. L., Sarmiento, J. L., Paynter, D. J., Dunne, J. P., Krasting, J. P. and Winton, M.: Dominance of the
553 Southern Ocean in Anthropogenic Carbon and Heat Uptake in CMIP5 Models, J. Clim., 28(2), 862–886,
554 doi:10/w3d, 2014.

Fukamachi, Y., Wakatsuchi, M., Taira, K., Kitagawa, S., Ushio, S., Takahashi, A., Oikawa, K., Furukawa, T., Yoritaka, H., Fukuchi, M. and Yamanouchi, T.: Seasonal variability of bottom water properties off Adélie Land, Antarctica, J. Geophys. Res. Oceans, 105(C3), 6531–6540, doi:10/c2fmvb, 2000.

Fukamachi, Y., Rintoul, S. R., Church, J. A., Aoki, S., Sokolov, S., Rosenberg, M. A. and Wakatsuchi, M.: Strong export of Antarctic Bottom Water east of the Kerguelen plateau, Nature Geoscience, 3, 327, doi:10/cqqpng, 2010.

Gattuso, J.-P. and Hansson, L.: Ocean Acidification, Oxford University Press, Oxford, New York., 2011.

Gibson, J. A. E. and Trull, T. W.: Annual cycle of fCO2 under sea-ice and in open water in Prydz Bay, East Antarctica, Mar. Chem., 66(3), 187–200, doi:10/fwg8ch, 1999.

Gordon, A. L.: Bottom Water Formation, in Encyclopedia of Ocean Sciences, pp. 334–340, Elsevier., 2001.

Gordon, A. L., Orsi, A. H., Muench, R., Huber, B. A., Zambianchi, E. and Visbeck, M.: Western Ross Sea continental slope gravity currents, Deep Sea Res. Part II Top. Stud. Oceanogr., 56(13), 796–817, doi:10/bhvf5c, 2009.

Gordon, A. L., Huber, B., McKee, D. and Visbeck, M.: A seasonal cycle in the export of bottom water from the Weddell Sea, Nature Geoscience, 3(8), 551–556, doi:10/bmwkr2, 2010.

Gordon, A. L., Huber, B. A. and Busecke, J.: Bottom water export from the western Ross Sea, 2007 through 2010, Geophys. Res. Lett., 42(13), 5387–5394, doi:10/f7k7xb, 2015.

Goyet, C., Adams, R. and Eischeid, G.: Observations of the CO2 system properties in the tropical Atlantic Ocean, Mar. Chem., 60(1), 49–61, doi:10/ckd593, 1998.

Gregor, L., Kok, S. and Monteiro, P. M. S.: Interannual drivers of the seasonal cycle of CO_2 in the Southern Ocean, Biogeosciences, 15(8), 2361–2378, doi:10/gddvp8, 2018.

Gruber, N.: Anthropogenic CO2 in the Atlantic Ocean, Glob. Biogeochem. Cycle, 12(1), 165–191, doi:10/d2d4v8, 1998.

Gruber, N., Gloor, M., Mikaloff Fletcher, S. E., Doney, S. C., Dutkiewicz, S., Follows, M. J., Gerber, M., Jacobson, A. R., Joos, F., Lindsay, K., Menemenlis, D., Mouchet, A., Müller, S. A., Sarmiento, J. L. and Takahashi, T.: Oceanic sources, sinks, and transport of atmospheric CO2, Glob. Biogeochem. Cycle, 23(1), doi:10/cf59hc, 2009.

Gruber, N., Clement, D., Carter, B. R., Feely, R. A., Heuven, S. van, Hoppema, M., Ishii, M., Key, R. M., Kozyr, A., Lauvset, S. K., Lo Monaco, C., Mathis, J. T., Murata, A., Olsen, A., Perez, F. F., Sabine, C. L., Tanhua, T. and Wanninkhof, R.: The oceanic sink for anthropogenic CO2 from 1994 to 2007, Science, 363(6432), 1193–1199, doi:10/gfw89w, 2019a.

Gruber, N., Landschützer, P. and Lovenduski, N. S.: The Variable Southern Ocean Carbon Sink, Annu. Rev. Mar. Sci., 11(1), 159–186, doi:10/gf7sc9, 2019b.

Hall, T. M., Haine, T. W. N. and Waugh, D. W.: Inferring the concentration of anthropogenic carbon in the ocean from tracers, Glob. Biogeochem. Cycle, 16(4), 78-1-78–15, doi:10/bd8qbz, 2002.

Hauck, J., Voelker, C., Wolf-Gladrow, D. A., Laufkoetter, C., Vogt, M., Aumont, O., Bopp, L., Buitenhuis, E. T., Doney, S. C., Dunne, J., Gruber, N., Hashioka, T., John, J., Le Quere, C., Lima, I. D., Nakano, H., Seferian, R. and Totterdell, I.: On the Southern Ocean CO2 uptake and the role of the biological carbon pump in the 21st century, Glob. Biogeochem. Cycle, 29(9), 1451–1470, doi:10/f7wkcs, 2015.

Heuzé, C., Heywood, K. J., Stevens, D. P. and Ridley, J. K.: Changes in Global Ocean Bottom Properties and Volume Transports in CMIP5 Models under Climate Change Scenarios, J. Clim., 28(8), 2917–2944, doi:10/f68qt7, 2014.

Heywood, K. J., Sparrow, M. D., Brown, J. and Dickson, R. R.: Frontal structure and Antarctic Bottom Water flow through the Princess Elizabeth Trough, Antarctica, Deep Sea Research Part I: Oceanographic Research Papers, 46(7), 1181–1200, doi:10/b6xbsv, 1999.

Ito, T., Bracco, A., Deutsch, C., Frenzel, H., Long, M. and Takano, Y.: Sustained growth of the Southern Ocean carbon storage in a warming climate, Geophys. Res. Lett., 42(11), 4516–4522, doi:10/f7jjrf, 2015.

Jabaud-Jan, A., Metzl, N., Brunet, C., Poisson, A. and Schauer, B.: Interannual variability of the carbon dioxide system in the southern Indian Ocean (20°S–60°S): The impact of a warm anomaly in austral summer 1998, Glob. Biogeochem. Cycle, 18(1), doi:10/fdtwhm, 2004.

Jiang, L.-Q., Carter, B. R., Feely, R. A., Lauvset, S. K. and Olsen, A.: Surface ocean pH and buffer capacity: past, present and future, Mar. Chem., 9(1), 1–11, doi:10/ggqvrs, 2019.

Johnson, G. C.: Quantifying Antarctic Bottom Water and North Atlantic Deep Water volumes, J. Geophys. Res. Oceans, 113(C5), doi:10/cx8cxn, 2008.

Johnson, G. C., Purkey, S. G. and Bullister, J. L.: Warming and Freshening in the Abyssal Southeastern Indian Ocean, J. Clim., 21(20), 5351–5363, doi:10/fmr6dk, 2008.

Kerr, R., Goyet, C., da Cunha, L. C., Orselli, I. B. M., Lencina-Avila, J. M., Mendes, C. R. B., Carvalho-Borges, M., Mata, M. M. and Tavano, V. M.: Carbonate system properties in the Gerlache Strait, Northern Antarctic Peninsula (February 2015): II. Anthropogenic CO2 and seawater acidification, Deep Sea Res. Part II Top. Stud. Oceanogr., 149, 182–192, doi:10/gf7sdh, 2018.

Key, R. M., Kozyr, A., Sabine, C. L., Lee, K., Wanninkhof, R., Bullister, J. L., Feely, R. A., Millero, F. J., Mordy, C. and Peng, T. H.: A global ocean carbon climatology: Results from Global Data Analysis Project (GLODAP), Glob. Biogeochem. Cycle, 18(4), GB4031, doi:10/dp7sk7, 2004.

Key, R. M., Tanhua, T., Olsen, A., Hoppema, M., Jutterström, S., Schirnick, C., van Heuven, S., Kozyr, A., Lin, X., Velo, A., Wallace, D. W. R., and Mintrop, L.: The CARINA data synthesis project: introduction and overview, Earth Syst. Sci. Data, 2, 105-121, doi:10.5194/essd-2-105-2010, 2010.

Key, R. M., Olsen, A., Van Heuven, S., Lauvset, S. K., Velo, A., Lin, X., Schirnick, C., Kozyr, A., Tanhua, T., Hoppema, M., Jutterstrom, S., Steinfeldt, R., Jeansson, E., Ishi, M., Perez, F. F. and Suzuki, T.: Global Ocean Data Analysis Project, Version 2 (GLODAPv2), ORNL/CDIAC-162, ND-P093, doi:10.3334/CDIAC/OTG.NDP093_GLODAPv2, 2015.

Khatiwala, S., Primeau, F. and Hall, T.: Reconstruction of the history of anthropogenic CO2 concentrations in the ocean, Nature, 462, 346, doi:10/fnz7f7, 2009.

Khatiwala, S., Tanhua, T., Mikaloff Fletcher, S., Gerber, M., Doney, S. C., Graven, H. D., Gruber, N., McKinley, G. A., Murata, A., Ríos, A. F. and Sabine, C. L.: Global ocean storage of anthropogenic carbon, Biogeosciences, 10(4), 2169–2191, doi:10/f4x3rw, 2013.

Körtzinger, A., Mintrop, L. and Duinker, J. C.: On the penetration of anthropogenic CO2 into the North Atlantic Ocean, J. Geophys. Res. Oceans, 103(C9), 18681–18689, doi:10/cjshtz, 1998.

Körtzinger, A., Rhein, M. and Mintrop, L.: Anthropogenic CO2 and CFCs in the North Atlantic Ocean - A comparison of man-made tracers, Geophys. Res. Lett., 26(14), 2065–2068, doi:10/c9xdbf, 1999.

Körtzinger, A., Hedges, J. I. and Quay, P. D.: Redfield ratios revisited: Removing the biasing effect of anthropogenic CO2, Limnol. Oceanogr., 46(4), 964–970, doi:10/dz32td, 2001.

Landschützer, P., Gruber, N., Haumann, F. A., Rödenbeck, C., Bakker, D. C. E., van Heuven, S., Hoppema, M., Metzl, N., Sweeney, C., Takahashi, T., Tilbrook, B. and Wanninkhof, R.: The reinvigoration of the Southern Ocean carbon sink, Science, 349(6253), 1221, doi:10/f7q9th, 2015.

Laruelle, G. G., Cai, W.-J., Hu, X., Gruber, N., Mackenzie, F. T. and Regnier, P.: Continental shelves as a variable but increasing global sink for atmospheric carbon dioxide, Nat. Commun., 9, 454, doi:10/gcxkgq, 2018.

Le Quéré, C., Rödenbeck, C., Buitenhuis, E. T., Conway, T. J., Langenfelds, R., Gomez, A., Labuschagne, C., Ramonet, M., Nakazawa, T., Metzl, N., Gillett, N. and Heimann, M.: Saturation of the Southern Ocean CO2 Sink Due to Recent Climate Change, Science, 316(5832), 1735, doi:10/fctrq9, 2007.

Le Quéré, C., Andrew, R. M., Friedlingstein, P., Sitch, S., Hauck, J., Pongratz, J., Pickers, P. A., Korsbakken, J. I., Peters, G. P., Canadell, J. G., Arneth, A., Arora, V. K., Barbero, L., Bastos, A., Bopp, L., Chevallier, F., Chini, L. P., Ciais, P., Doney, S. C., Gkritzalis, T., Goll, D. S., Harris, I., Haverd, V., Hoffman, F. M., Hoppema, M., Houghton, R. A., Hurtt, G., Ilyina, T., Jain, A. K., Johannessen, T., Jones, C. D., Kato, E., Keeling, R. F., Goldewijk, K. K., Landschützer, P., Lefèvre, N., Lienert, S., Liu, Z., Lombardozzi, D., Metzl, N., Munro, D. R., Nabel, J. E. M. S., Nakaoka, S., Neill, C., Olsen, A., Ono, T., Patra, P., Peregon, A., Peters, W., Peylin, P., Pfeil, B., Pierrot, D., Poulter, B., Rehder, G., Resplandy, L., Robertson, E., Rocher, M., Rödenbeck, C., Schuster, U., Schwinger, J., Séférian, R., Skjelvan, I., Steinhoff, T., Sutton, A., Tans, P. P., Tian, H., Tilbrook, B., Tubiello, F. N., Laan-Luijkx, I. T. van der, Werf, G. R. van der, Viovy, N., Walker, A. P., Wiltshire, A. J., Wright, R., Zaehle, S. and Zheng, B.: Global Carbon Budget 2018, Earth Syst. Sci. Data, 10(4), 2141–2194, doi:10/gfn48b, 2018.

Lenton, A., Metzl, N., Takahashi, T., Kuchinke, M., Matear, R. J., Roy, T., Sutherland, S. C., Sweeney, C. and Tilbrook, B.: The observed evolution of oceanic pCO(2) and its drivers over the last two decades, Glob. Biogeochem. Cycle, 26, GB2021, doi:10/gf7sd3, 2012.

Lo Monaco, C., Metzl, N., Poisson, A., Brunet, C. and Schauer, B.: Anthropogenic CO2 in the Southern Ocean: Distribution and inventory at the Indian-Atlantic boundary (World Ocean Circulation Experiment line I6), J. Geophys. Res. Oceans, 110(C6), doi:10/crcngf, 2005a.

Lo Monaco, C., Goyet, C., Metzl, N., Poisson, A. and Touratier, F.: Distribution and inventory of anthropogenic CO2 in the Southern Ocean: Comparison of three data-based methods, J. Geophys. Res. Oceans, 110(C9), doi:10/d554k3, 2005b.

Lo Monaco, C., Álvarez, M., Key, R. M., Lin, X., Tanhua, T., Tilbrook, B., Bakker, D. C., Van Heuven, S., Hoppema, M. and Metzl, N.: Assessing the internal consistency of the CARINA database in the Indian sector of the Southern Ocean, Earth Syst. Sci. Data, 2(1), 51–70, doi:10/dtcv57, 2010.

Mantyla, A. and Reid, J.: On the Origins of Deep and Bottom Waters of the Indian-Ocean, J. Geophys. Res. Oceans, 100(C2), 2417–2439, doi:10/cb6r8m, 1995.

Marshall, J. and Speer, K.: Closure of the meridional overturning circulation through Southern Ocean upwelling, Nature Geoscience, 5(3), 171–180, doi:10/gf7sc5, 2012.

Matear, R. J.: Effects of numerical advection schemes and eddy parameterizations on ocean ventilation and oceanic anthropogenic CO2 uptake, Ocean Modelling, 3(3), 217–248, doi:10/b4t667, 2001.

McKee, D. C., Yuan, X., Gordon, A. L., Huber, B. A. and Dong, Z.: Climate impact on interannual variability of Weddell Sea Bottom Water, J. Geophys. Res. Oceans, 116(C5), doi:10/cfcfb6, 2011.

McNeil, B. I., Matear, R. J., Key, R. M., Bullister, J. L. and Sarmiento, J. L.: Anthropogenic CO_2 Uptake by the Ocean Based on the Global Chlorofluorocarbon Data Set, Science, 299(5604), 235, doi:10/bpv29x, 2003.

Meijers, A. J. S., Klocker, A., Bindoff, N. L., Williams, G. D. and Marsland, S. J.: The circulation and water masses of the Antarctic shelf and continental slope between 30 and 80∘E, Deep Sea Res. Part II Top. Stud. Oceanogr., 57(9), 723–737, doi:10/c8qn5g, 2010.

Menezes, V. V., Macdonald, A. M. and Schatzman, C.: Accelerated freshening of Antarctic Bottom Water over the last decade in the Southern Indian Ocean, Sci. Adv., 3(1), e1601426, doi:10/gf7sbh, 2017.

Metzl, N.: Decadal increase of oceanic carbon dioxide in Southern Indian Ocean surface waters (1991–2007), Deep Sea Res. Part II Top. Stud. Oceanogr., 56(8), 607–619, doi:10/ff939g, 2009.

Metzl, N., Brunet, C., Jabaud-Jan, A., Poisson, A. and Schauer, B.: Summer and winter air–sea CO2 fluxes in the Southern Ocean, Deep Sea Res. Pt. I Oceanogr. Res. Pap., 53(9), 1548–1563, doi:10/c29cmm, 2006.

683 Munro, D. R., Lovenduski, N. S., Takahashi, T., Stephens, B. B., Newberger, T. and Sweeney, C.: Recent evidence
684 for a strengthening CO2 sink in the Southern Ocean from carbonate system measurements in the Drake Passage
685 (2002-2015), Geophys. Res. Lett., 42(18), 7623–7630, doi:10/gf7sd4, 2015.

686 Murata, A., Kumamoto, Y. and Sasaki, K.: Decadal-Scale Increase of Anthropogenic CO2 in Antarctic Bottom
687 Water in the Indian and Western Pacific Sectors of the Southern Ocean, Geophys. Res. Lett., 46(2), 833–841,
688 doi:10/gfkpzq, 2019.

689 Ohshima, K. I., Fukamachi, Y., Williams, G. D., Nihashi, S., Roquet, F., Kitade, Y., Tamura, T., Hirano, D.,
690 Herraiz-Borreguero, L., Field, I., Hindell, M., Aoki, S. and Wakatsuchi, M.: Antarctic Bottom Water production
691 by intense sea-ice formation in the Cape Darnley polynya, Nature Geoscience, 6(3), 235–240, doi:10/f22qfg, 2013.

692 Olsen, A., Key, R. M., van Heuven, S., Lauvset, S. K., Velo, A., Lin, X., Schirnick, C., Kozyr, A., Tanhua, T.,
693 Hoppema, M., Jutterström, S., Steinfeldt, R., Jeansson, E., Ishii, M., Pérez, F. F. and Suzuki, T.: The Global Ocean
694 Data Analysis Project version 2 (GLODAPv2) – an internally consistent data product for the world ocean, Earth
695 Syst. Sci. Data, 8(2), 297–323, doi:10/f8377c, 2016.

696 Olsen, A., Lange, N., Key, R. M., Tanhua, T., Álvarez, M., Becker, S., Bittig, H. C., Carter, B. R., Cotrim da
697 Cunha, L., Feely, R. A., Heuven, S. van, Hoppema, M., Ishii, M., Jeansson, E., Jones, S. D., Jutterström, S.,
698 Karlsen, M. K., Kozyr, A., Lauvset, S. K., Lo Monaco, C., Murata, A., Pérez, F. F., Pfeil, B., Schirnick, C.,
699 Steinfeldt, R., Suzuki, T., Telszewski, M., Tilbrook, B., Velo, A. and Wanninkhof, R.: GLODAPv2.2019 – an
700 update of GLODAPv2, Earth Syst. Sci. Data, 11(3), 1437–1461, doi:10/ggrh7d, 2019.

701 Orr, J. C., Maier-Reimer, E., Mikolajewicz, U., Monfray, P., Sarmiento, J. L., Toggweiler, J. R., Taylor, N. K.,
702 Palmer, J., Gruber, N., Sabine, C. L., Quéré, C. L., Key, R. M. and Boutin, J.: Estimates of anthropogenic carbon
703 uptake from four three-dimensional global ocean models, Glob. Biogeochem. Cycle, 15(1), 43–60, doi:10/chb7qz,
704 2001.

705 Orr, J. C., Fabry, V. J., Aumont, O., Bopp, L., Doney, S. C., Feely, R. A., Gnanadesikan, A., Gruber, N., Ishida,
706 A., Joos, F., Key, R. M., Lindsay, K., Maier-Reimer, E., Matear, R., Monfray, P., Mouchet, A., Najjar, R. G.,
707 Plattner, G.-K., Rodgers, K. B., Sabine, C. L., Sarmiento, J. L., Schlitzer, R., Slater, R. D., Totterdell, I. J., Weirig,
708 M.-F., Yamanaka, Y. and Yool, A.: Anthropogenic ocean acidification over the twenty-first century and its impact
709 on calcifying organisms, Nature, 437(7059), 681–686, doi:10/fss432, 2005.

710 Orsi, A. H., Johnson, G. C. and Bullister, J. L.: Circulation, mixing, and production of Antarctic Bottom Water,
711 Prog. Oceanogr., 43(1), 55–109, doi:10/c7n7mx, 1999.

712 Pardo, P. C., Pérez, F. F., Khatiwala, S. and Ríos, A. F.: Anthropogenic CO2 estimates in the Southern Ocean:
713 Storage partitioning in the different water masses, Prog. Oceanogr., 120, 230–242, doi:10/f5r3v3, 2014.

714 Pardo, P. C., Tilbrook, B., Langlais, C., Trull, T. W. and Rintoul, S. R.: Carbon uptake and biogeochemical change
715 in the Southern Ocean, south of Tasmania, Biogeosciences, 14(22), 5217–5237, doi:10/gcmq92, 2017.

716 Poisson, A. and Chen, C.-T. A.: Why is there little anthropogenic CO2 in the Antarttic bottom water?, Deep Sea
717 Res. Part A Oceanogr. Res. Pap., 34(7), 1255–1275, doi:10/bq8cdr, 1987.

718 Purkey, S. G. and Johnson, G. C.: Warming of Global Abyssal and Deep Southern Ocean Waters between the
719 1990s and 2000s: Contributions to Global Heat and Sea Level Rise Budgets, J. Clim., 23(23), 6336–6351,
720 doi:10/dqf7tx, 2010.

721 Purkey, S. G. and Johnson, G. C.: Global Contraction of Antarctic Bottom Water between the 1980s and 2000s, J.
722 Clim., 25(17), 5830–5844, doi:10/f39bks, 2012.

723 Ridgwell, A. and Zeebe, R. E.: The role of the global carbonate cycle in the regulation and evolution of the Earth
724 system, Earth Planet. Sci. Lett., 234(3), 299–315, doi:10/fcp4bw, 2005.

725 Rintoul, S.R., Sparrow, M., Meredith, M.P., Wadley, V., Speer, K., Hofmann, E., Summerhayes, C., Urban, E.,
726 and Bellerby, R.: The Southern Ocean Observing System: Initial Science and Implementation Strategy. Scientific
727 Committee on Antarctic Research/Scientific Committee on Oceanic Research, 74 pp., 2012.

728 Rintoul, S. R.: Rapid freshening of Antarctic Bottom Water formed in the Indian and Pacific oceans, Geophys.
729 Res. Lett., 34(6), L06606, doi:10/dqswfv, 2007.

730 Rios, A. F., Velo, A., Pardo, P. C., Hoppema, M. and Perez, F. F.: An update of anthropogenic CO2 storage rates
731 in the western South Atlantic basin and the role of Antarctic Bottom Water, J. Mar. Syst., 94, 197–203,
732 doi:10/csg8gp, 2012.

733 Robertson, R., Visbeck, M., Gordon, A. L. and Fahrbach, E.: Long-term temperature trends in the deep waters of
734 the Weddell Sea, Deep Sea Res. Part II Top. Stud. Oceanogr., 49(21), 4791–4806, doi:10/fkm6j2, 2002.

735 Rodehacke, C. B., Hellmer, H. H., Beckmann, A. and Roether, W.: Formation and spreading of Antarctic deep
736 and bottom waters inferred from a chlorofluorocarbon (CFC) simulation, J. Geophys. Res. Oceans, 112(C9),
737 doi:10/dmrrts, 2007.

738 Roden, N. P., Shadwick, E. H., Tilbrook, B. and Trull, T. W.: Annual cycle of carbonate chemistry and decadal
739 change in coastal Prydz Bay, East Antarctica, Mar. Chem., 155, 135–147, doi:10/f5czpc, 2013.

740 Roden, N. P., Tilbrook, B., Trull, T. W., Virtue, P. and Williams, G. D.: Carbon cycling dynamics in the seasonal
741 sea-ice zone of East Antarctica, J. Geophys. Res. Oceans, 121(12), 8749–8769, doi:10/f9pzpx, 2016.

742 Russell, J. L., Kamenkovich, I., Bitz, C., Ferrari, R., Gille, S. T., Goodman, P. J., Hallberg, R., Johnson, K.,
743 Khazmutdinova, K., Marinov, I., Mazloff, M., Riser, S., Sarmiento, J. L., Speer, K., Talley, L. D. and Wanninkhof,
744 R.: Metrics for the Evaluation of the Southern Ocean in Coupled Climate Models and Earth System Models, J.
745 Geophys. Res. Oceans, 123(5), 3120–3143, doi:10/gdjzgh, 2018.

Sabine, C. L., Key, R. M., Johnson, K. M., Millero, F. J., Poisson, A., Sarmiento, J. L., Wallace, D. W. R. and Winn, C. D.: Anthropogenic CO2 inventory of the Indian Ocean, Glob. Biogeochem. Cycle, 13(1), 179–198, doi:10/cz2xzm, 1999.

Sabine, C. L., Feely, R. A., Gruber, N., Key, R. M., Lee, K., Bullister, J. L., Wanninkhof, R., Wong, C. S., Wallace, D. W. R., Tilbrook, B., Millero, F. J., Peng, T.-H., Kozyr, A., Ono, T. and Rios, A. F.: The Oceanic Sink for Anthropogenic CO2, Science, 305(5682), 367–371, doi:10/cbg2cq, 2004.

Sandrini, S., Ait-Ameur, N., Rivaro, P., Massolo, S., Touratier, F., Tositti, L. and Goyet, C.: Anthropogenic carbon distribution in the Ross Sea, Antarctica, Antarct. Sci, 19(3), 395–407, doi:10/b3jnjp, 2007.

Schlitzer, R., Ocean data view, http://odv.awi.de, 2019.

Schmidtko, S., Stramma, L. and Visbeck, M.: Decline in global oceanic oxygen content during the past five decades, Nature, 542, 335, doi:10/f9qh2h, 2017.

Shadwick, E. H., Rintoul, S. R., Tilbrook, B., Williams, G. D., Young, N., Fraser, A. D., Marchant, H., Smith, J. and Tamura, T.: Glacier tongue calving reduced dense water formation and enhanced carbon uptake, Geophys. Res. Lett., 40(5), 904–909, doi:10/gf7sd5, 2013.

Shadwick, E. H., Tilbrook, B. and Williams, G. D.: Carbonate chemistry in the Mertz Polynya (East Antarctica): Biological and physical modification of dense water outflows and the export of anthropogenic CO2, J. Geophys. Res. Oceans, 119(1), 1–14, doi:10/f5vcvw, 2014.

Siegenthaler, U. and Sarmiento, J. L.: Atmospheric carbon dioxide and the ocean, Nature, 365, 119, doi:10/fq9bjr, 1993.

Smith, N. and Treguer, P.: Physical and Chemical Oceanography in the Vicinity of Prydz Bay, Antarctica, edited by S. Z. ElSayed, Cambridge Univ Press, Cambridge., 1994.

Takahashi, T., Sutherland, S. C., Wanninkhof, R., Sweeney, C., Feely, R. A., Chipman, D. W., Hales, B., Friederich, G., Chavez, F., Sabine, C., Watson, A., Bakker, D. C. E., Schuster, U., Metzl, N., Yoshikawa-Inoue, H., Ishii, M., Midorikawa, T., Nojiri, Y., Koertzinger, A., Steinhoff, T., Hoppema, M., Olafsson, J., Arnarson, T. S., Tilbrook, B., Johannessen, T., Olsen, A., Bellerby, R., Wong, C. S., Delille, B., Bates, N. R. and de Baar, H. J. W.: Climatological mean and decadal change in surface ocean pCO(2), and net sea-air CO2 flux over the global oceans, Deep-Sea Res. Part II-Top. Stud. Oceanogr., 56(8–10), 554–577, doi:10/b77k3p, 2009.

Takahashi, T., Sweeney, C., Hales, B., Chipman, D. W., Newberger, T., Goddard, J. G., Iannuzzi, R. A. and Sutherland, S. C.: The Changing Carbon Cycle in the Southern Ocean, Oceanography, 25(3), 26–37, doi:10/f4bpqs, 2012.

Tamura, T., Ohshima, K. I., Fraser, A. D. and Williams, G. D.: Sea ice production variability in Antarctic coastal polynyas, J. Geophys. Res. Oceans, 121(5), 2967–2979, doi:10/f85drd, 2016.

778 Touratier, F. and Goyet, C.: Applying the new TrOCA approach to assess the distribution of anthropogenic CO2
779 in the Atlantic Ocean, J. Mar. Syst., 46(1), 181–197, doi:10/dm85j9, 2004a.

780 Touratier, F. and Goyet, C.: Definition, properties, and Atlantic Ocean distribution of the new tracer TrOCA, J.
781 Mar. Syst., 46(1), 169–179, doi:10/br4x3b, 2004b.

782 Touratier, F., Azouzi, L. and Goyet, C.: CFC-11, Δ14C and 3H tracers as a means to assess anthropogenic CO2
783 concentrations in the ocean, Tellus B Chem. Phys. Meteorol., 59(2), 318–325, doi:10.1111/j.1600-
784 0889.2006.00247.x, 2007.

785 Tréguer, P., and P. Le Corre: Manuel d'analyse des sels nutritifs dans l'eau de mer (utilisation de l'autoanalyseur
786 II Technicon), 2nd ed., 110 pp., L.O.C.U.B.O., Brest, 1975.

787 van Heuven, S. M. A. C., Hoppema, M., Huhn, O., Slagter, H. A. and de Baar, H. J. W.: Direct observation of
788 increasing CO2 in the Weddell Gyre along the Prime Meridian during 1973–2008, Deep Sea Res. Part II Top.
789 Stud. Oceanogr., 58(25), 2613–2635, doi:10/fh9jvz, 2011.

790 van Heuven, S. M. A. C.: Determination of the rate of oceanic storage of anthropogenic CO2 from measurements
791 in the ocean interior: The South Atlantic Ocean, Doctor of Philosophy, Groningen, 2013.

792 van Heuven, S. M. A. C., Hoppema, M., Jones, E. M. and de Baar, H. J. W.: Rapid invasion of anthropogenic CO2
793 into the deep circulation of the Weddell Gyre, Phil. Trans. R. Soc. A ou Philos. Trans. R. Soc. A-Math. Phys. Eng.
794 Sci., 372(2019), 20130056, doi:10/gf7sc6, 2014.

795 Van Wijk, E. M. and Rintoul, S. R.: Freshening drives contraction of Antarctic Bottom Water in the Australian
796 Antarctic Basin, Geophys. Res. Lett., 41(5), 1657–1664, doi:10/f5x9ff, 2014.

797 Vázquez-Rodríguez, M., Touratier, F., Lo Monaco, C., Waugh, D. W., Padin, X. A., Bellerby, R. G. J., Goyet, C.,
798 Metzl, N., Ríos, A. F. and Pérez, F. F.: Anthropogenic carbon distributions in the Atlantic Ocean: data-based
799 estimates from the Arctic to the Antarctic, Biogeosciences, 6(3), 439–451, doi:10/d8scnn, 2009.

800 Waugh, D. W., Hall, T. M., Mcneil, B. I., Key, R. and Matear, R. J.: Anthropogenic CO2 in the oceans estimated
801 using transit time distributions, Tellus B Chem. Phys. Meteorol., 58(5), 376–389, doi:10/bdx89x, 2006.

802 Weiss, R. F.: The solubility of nitrogen, oxygen and argon in water and seawater, Deep Sea Res. and Oceanogr.
803 Abs., 17(4), 721–735, doi:10/dxzznb, 1970.

804 Williams, G. D., Bindoff, N. L., Marsland, S. J. and Rintoul, S. R.: Formation and export of dense shelf water from
805 the Adelie Depression, East Antarctica, J. Geophys. Res. Oceans, 113(C4), C04039, doi:10/cp99bm, 2008.

806 Williams, G. D., Aoki, S., Jacobs, S. S., Rintoul, S. R., Tamura, T. and Bindoff, N. L.: Antarctic Bottom Water
807 from the Adélie and George V Land coast, East Antarctica (140–149°E), J. Geophys. Res. Oceans, 115(C4),
808 doi:10/c38prf, 2010.

Williams, G. D., Herraiz-Borreguero, L., Roquet, F., Tamura, T., Ohshima, K. I., Fukamachi, Y., Fraser, A. D., Gao, L., Chen, H., McMahon, C. R., Harcourt, R. and Hindell, M.: The suppression of Antarctic bottom water formation by melting ice shelves in Prydz Bay, Nat. Commun., 7, 12577, doi:10/f3sfx9, 2016.

Williams, N. L., Feely, R. A., Sabine, C. L., Dickson, A. G., Swift, J. H., Talley, L. D. and Russell, J. L.: Quantifying anthropogenic carbon inventory changes in the Pacific sector of the Southern Ocean, Mar. Chem., 174, 147–160, doi:10/f7mghw, 2015.

Williams, N. L., Juranek, L. W., Feely, R. A., Russell, J. L., Johnson, K. S. and Hales, B.: Assessment of the Carbonate Chemistry Seasonal Cycles in the Southern Ocean From Persistent Observational Platforms, J. Geophys. Res. Oceans, 123(7), 4833–4852, doi:10/gd5tj8, 2018.

Williams, W. J., Carmack, E. C. and Ingram, R. G.: Physical Oceanography of Polynyas, in Polynyas: Windows to the World, vol. 74, edited by W. O. Smith and D. G. Barber, pp. 55–85, Elsevier Science Bv, Amsterdam., 2007.

Yabuki, T., Suga, T., Hanawa, K., Matsuoka, K., Kiwada, H. and Watanabe, T.: Possible source of the antarctic bottom water in the Prydz Bay Region, J. Oceanogr., 62(5), 649, doi:10/cbsxh9, 2006.

Yamamoto, A., Abe-Ouchi, A., Shigemitsu, M., Oka, A., Takahashi, K., Ohgaito, R. and Yamanaka, Y.: Global deep ocean oxygenation by enhanced ventilation in the Southern Ocean under long-term global warming, Glob. Biogeochem. Cycle, 29(10), 1801–1815, doi:10/f7xnvd, 2015.

Table 1. List of the cruises used in this study.

Cruise	Station	Location	Year	Month
GEOSECS	430	61.0°E / 60.0°S	1978	February
INDIGO-1	14	58.9°E / 53.0°S	1985	March
INDIGO-3	75	63.2°E / 56.5°S	1987	January
OISO-01	11	63.0°E / 56.5°S	1998	February
OISO-03	11	63.0°E / 56.5°S	1998	December
OISO-05	11	63.0°E / 56.5°S	2000	August
OISO-06	11	63.0°E / 56.5°S	2001	January
OISO-08	11	63.0°E / 56.5°S	2002	January
OISO-11	11	63.0°E / 56.5°S	2004	January
OISO-18	11	63.0°E / 56.5°S	2009	December
OISO-19	11	63.0°E / 56.5°S	2011	January
OISO-21	11	63.0°E / 56.5°S	2012	February
OISO-23	11	63.0°E / 56.5°S	2014	January
OISO-26	11	63.0°E / 56.5°S	2016	October
OISO-27	11	63.0°E / 56.5°S	2017	January
OISO-28	11	63.0°E / 56.5°S	2018	January

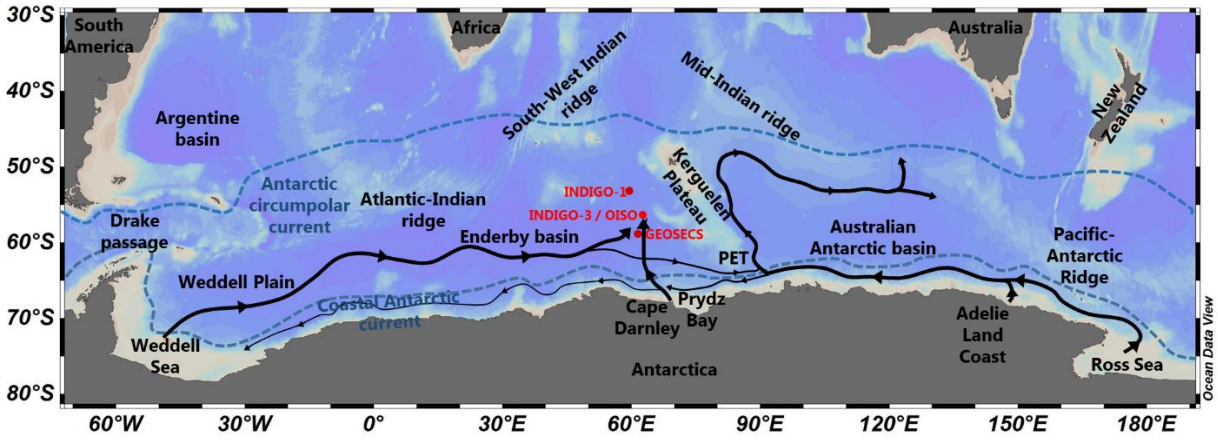

Figure 1. The AABWs circulation from the literature (Fukamachi et al., 2010; Orsi et al., 1999) and this study, with geographic indications (black text), SO currents (blue text and dash lines for the approximative positions) and stations considered in this study (red text and dots). PET: Princess Elizabeth Trough. Figure produced with ODV (Schlitzer et al., 2019).

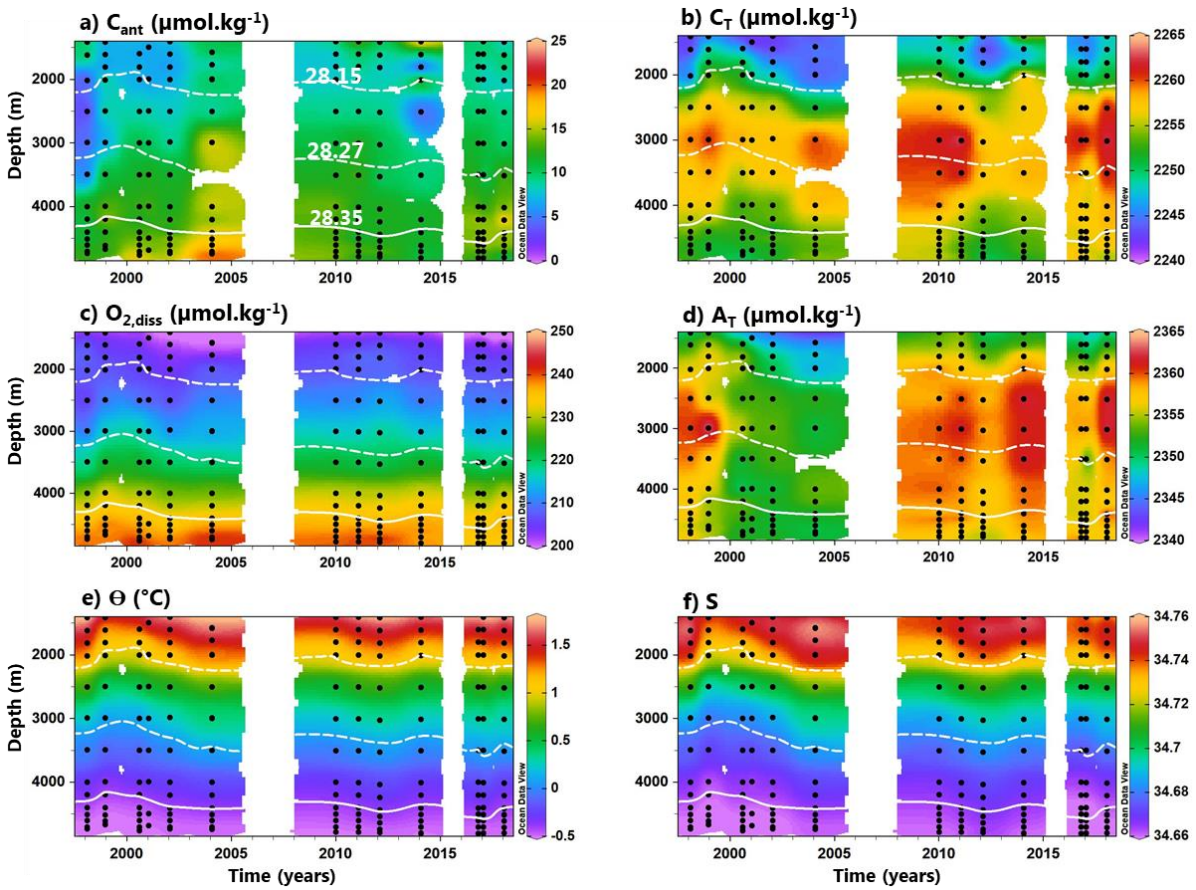

847

848 **Figure 2. Hovmöller section of (a) C_{ant} via TrOCA, (b) C_T, (c) O_2, (d) A_T, (e) θ and (f) S based on the OISO data presented**
849 **in Table 1. Data points are represented by black dots. The white isolines represent the water masses separation by γ^n**
850 **(from the bottom: LAABW, UAABW and LCDW). Figure produced with ODV (Schlitzer et al., 2019).**

851

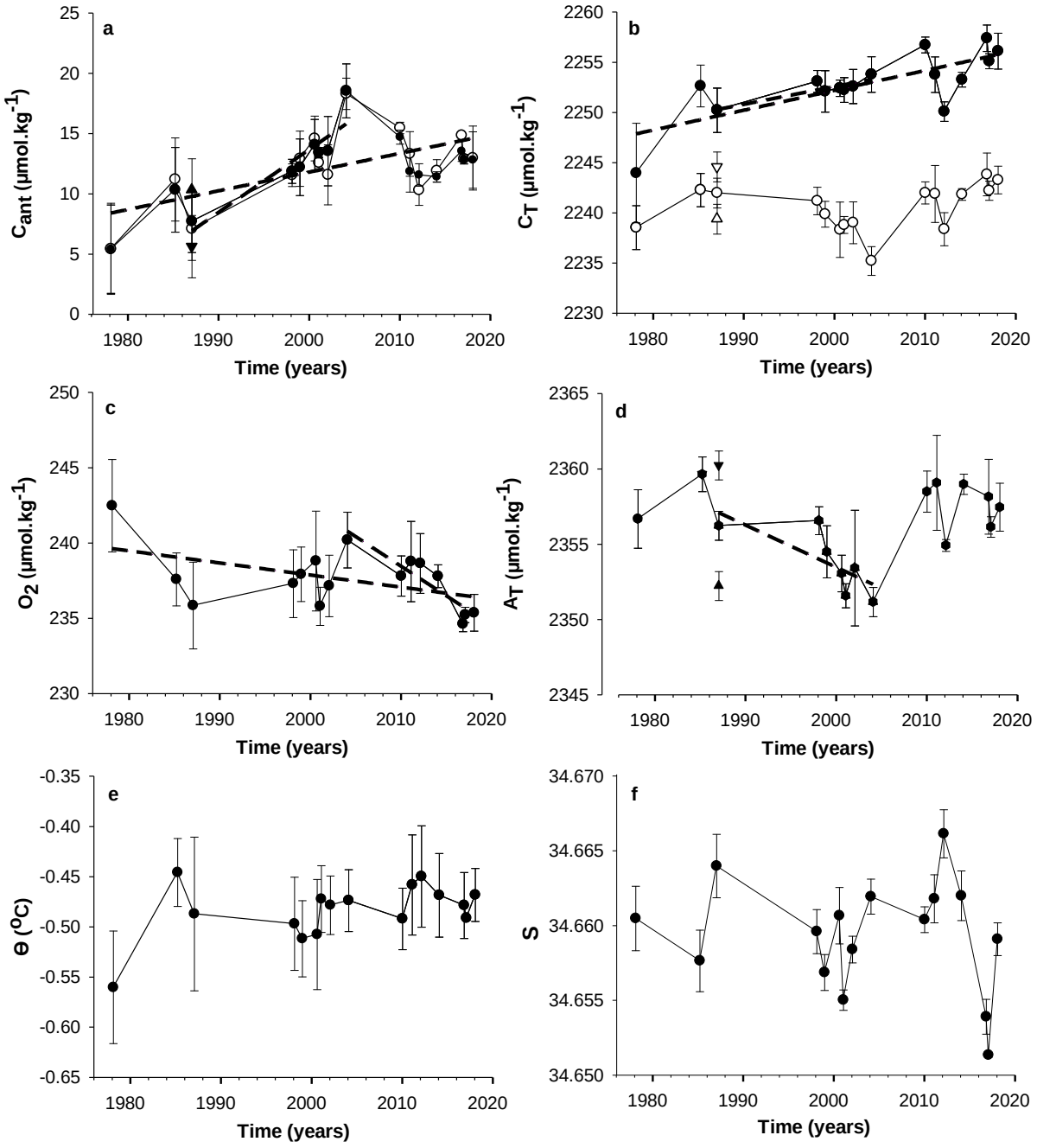

Figure 3. Interannual variability (dash lines lines) and significant trends (at 95 %, see Table 2; dotted lines) for the 40 years of observation of the OISO-ST11 LAABW properties, including (a) C_{ant} by the TrOCA (black circles and triangles) and the C^0 (open circles) method, (b) C_T (black circles) and C_{nat} (open circles), (c) O_2, (d) A_T, (e) Θ and (f) S. For (a) C_{ant}, (b) C_{nat} and (d) A_T, the triangles pointing down and up correspond to INDIGO-3 value without and with -8 µmol.kg^{-1} of correction on the A_T, respectively (see Supp. Mat. for more details).

Table 2: Trends (per decade) of observed and calculated properties in the LAABW estimated over different periods (in bold: significant trends at 95 % confidence level).

Period	S	Θ °C	Si µmol.kg^{-1}	NO_3 µmol.kg^{-1}	O_2 µmol.kg^{-1}	A_T µmol.kg^{-1}	C_T µmol.kg^{-1}	C_{ant} TrOCA µmol.kg^{-1}
1978-2018	-0.001 ± 0.001	0.01 ± 0.01	-1.2 ± 0.9	0.2 ± 0.2	**-0.8 ± 0.4**	-0.1 ± 0.1	**2.0 ± 0.5**	**1.4 ± 0.5**
1987-2018	-0.001 ± 0.001	0.01 ± 0.01	-1.9 ± 1.4	0.3 ± 0.4	-0.3 ± 0.5	0.6 ± 0.1	**1.6 ± 0.5**	1.1 ± 0.8
1987-2004	-0.003 ± 0.002	0.01 ± 0.01	**-6.5 ± 1.8**	0.9 ± 0.9	1.7 ± 1.0	**-1.9 ± 1.1**	**1.8 ± 0.4**	**5.2 ± 1.1**
2004-2018	-0.006 ± 0.003	0.01 ± 0.01	-1.8 ± 4.5	-0.5 ± 1.0	**-3.9 ± 0.7**	3.4 ± 0.2	1.7 ± 1.9	-3.5 ± 1.5

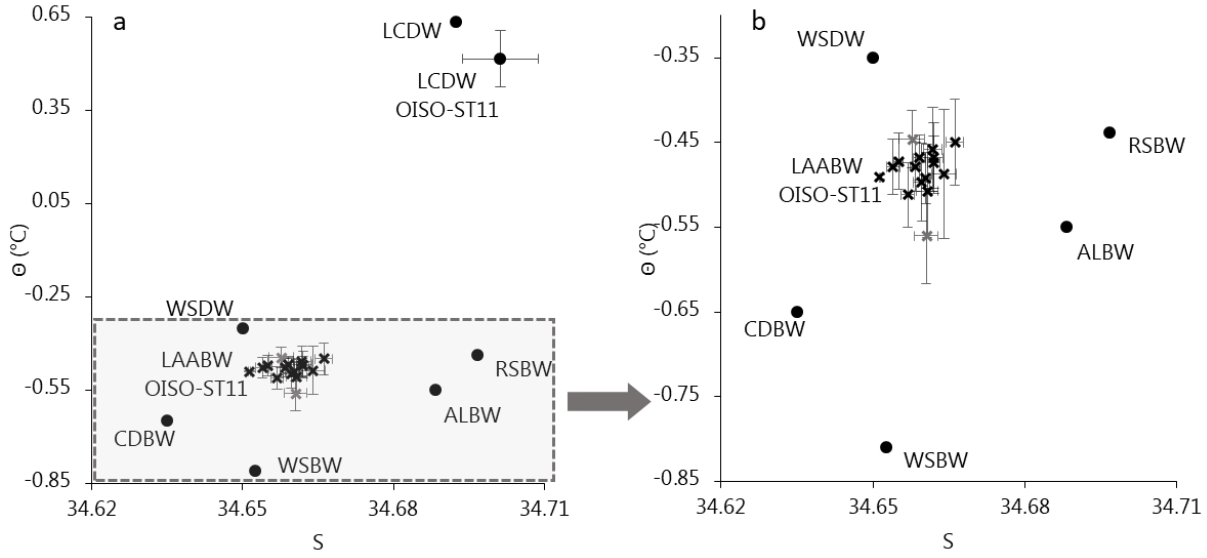

Figure 4. (a) Full Θ-S diagram of studied water masses and (b) zoomed on bottom waters. Values are from literature for the WSBW (Fukamachi et al., 2010; van Heuven, 2013; Pardo et al., 2014; Robertson et al., 2002), the WSDW (Carmack and Foster, 1975; Fahrbach et al., 1994; van Heuven, 2013; Robertson et al., 2002), the RSBW (Fukamachi et al., 2010; Gordon et al., 2015; Johnson, 2008; Pardo et al., 2014), the ALBW (Fukamachi et al., 2010; Johnson, 2008; Pardo et al., 2014), the CDBW (Ohshima et al., 2013) and the LCDW (Lo Monaco et al., 2005a; Pardo et al., 2014; Smith and Treguer, 1994), and from the OISO-ST11 dataset for the OISO-ST11 LAABW and OISO-ST11 LCDW. Error bars are calculated from the individual annual averaged values for the OISO-ST11 LAABW and from all data for the OISO-ST11 LCDW. For the OISO-ST11 LAABW, the grey cross are the GEOSECS (lowest Θ) and INDIGO-1 (highest Θ) values.

882 **Table 3. Compilation of C_{ant} sequestration investigations in the AABWs ($\gamma^n \geq 28.25$ kg.m^{-3}) using the TrOCA method.**
883 **The C_{ant} estimation of Pardo et al. (2014) is calculated using theoretical AABW mean composition (with 3% of ALBW)**
884 **and the carbon data from the GLODAPv1 and CARINA databases. Sandrini et al. (2007) values has been measured at**
885 **the bottom in the Ross Sea and correspond to recently sink high salinity surface water. The mean values published by**
886 **Roden et al. (2016) for the AABWs present WSDW characteristics but can be a mix of CDBW and LCDW.**

Source	Location	Water masses considered	Year	C_{ant} µmol.kg^{-1}
Pardo et al. (2014) Fig. 5	Averaged AABW composition	WSBW-RSBW-ALBW	1994	12
Lo Monaco et al. (2005b) Fig. 4b	WOCE line I6 (30°E; 50°-70°S)	WSBW CDBW	1996	15 20
Sandrini et al. (2007) Fig. 4a	Ross Sea	HSSW (previous RSBW)	2002/2003	Max. of 30
Shadwick et al. (2014) Table 2	Mertz polynya and Adelie depression	ALBW	2007/2008	15
Roden et al. (2016) Table 2	South Indian ocean (30°-80°E; 60°-69°S)	WSDW-LCDW-CDBW	2006	25
van Heuven et al. (2011) Fig.13	Weddell gyre (0°E; 55°-71°S)	WSBW	2005	16
This study	Enderby basin (56.5°S-63°E)	WSDW-CDBW-RSBW-ALBW	1978-1987	8 ± 3
			1987-1998	10 ± 4
			1987-2004	13 ± 4
			1998-2004	14 ± 2
			2010-2018	13 ± 1
			1978-2018	**12 ± 3**

887